UKNDC(74)-P-63

UNCLASSIFIED

UKNDC (74) P63
NEANDC (UK) 160L
INDC (UK) - 23/L
INDC-649

U.K. NUCLEAR DATA PROGRESS REPORT

April 1973 - March 1974

Editor M.G. Sowerby

Nuclear Physics Division,
AERE HARWELL.

July 1974

HL.74/2908
HMD.

PREFACE

This report is prepared at the request of the United Kingdom Nuclear Data Committee. It brings together reports on Nuclear Data from Harwell, Winfrith, Aldermaston, Dounreay, the National Physical Laboratory, the Berkeley Nuclear Laboratory of the Central Electricity Generating Board and the University of Glasgow. Most of the reports are presented under a laboratory heading but it is more convenient to present those contributions on Chemical Nuclear Data under a heading of that name. Where the work is relevant to requests in WRENDA 74 (INDC (SEC) - 38U) the appropriate request numbers are listed after the title of the contribution. A CINDA type index is included in the front of the document.

Element S	A	Quantity	Type	Energy Min.	Energy Max.	Documentation Ref.	Vol.	Page	Date	Lab.	Comments
H	1	DIFF ELASTIC	EXPT-PROG	1.4 7	2.8 7	UKNDC	P63	50	7/74	HAR	COOKSON+ SCAT INTO FORWARD HEMIS TBC
HE	3	EVALUATION	EVAL-PROG			UKNDC	P63	55	7/74	WIN	STORY+ TBC
LI	6	RESON PARAMS	EXPT-PROG	2.5 5		UKNDC	P63	23	7/74	HAR	UTTLEY+ OKS LINAC MEAS RESON ENERGY
C		THRMLSCAT LAW	EVAL-PROG			UKNDC	P63	55	7/74	WIN	BUTLAND EVAL IMPROVES REACTOR CALC
MG		EVALUATION	EVAL-PROG			UKNDC	P63	55	7/74	WIN	STORY+ TBC
AL	27	EVALUATION	EVAL-PROG			UKNDC	P63	55	7/74	WIN	STORY+ FILE AVAILABLE DFN 935
FE		TOTAL XSECT	EXPT-PROG	1.0 3	1.0 6	UKNDC	P63	37	7/74	HAR	BOWEN+ TOF CYCLOTRON RESON ANAL TBC
NI		TOTAL XSECT	EXPT-PROG	1.0 3	1.0 6	UKNDC	P63	37	7/74	HAR	BOWEN+ TOF CYCLOTRON RESON ANAL TBC
Nb	93	SPECT NGAMMA	EXPT-PROG	1.0 2	3.8 3	UKNDC	P63	27	7/74	HAR	THOMAS+ TOF LINAC CORR ANAL
Nb	93	RESON PARAMS	EXPT-PROG	3.6 1	1.0 3	UKNDC	P63	27	7/74	HAR	THOMAS+ J FOR 11 P-WAVE RES TBL
RH	103	SPECT NGAMMA	EXPT-PROG		1.0 3	UKNDC	P63	27	7/74	HAR	THOMAS+ TOF LINAC TBC
IN		EVALUATION	EVAL-PROG			UKNDC	P63	55	7/74	WIN	STORY+ TBC
SN		EVALUATION	EVAL-PROG			UKNDC	P63	55	7/74	WIN	STORY+ TBC
LA		TOTAL XSECT	EXPT-PROG	7.0 5	9.0 6	UKNDC	P63	62	7/74	GLS	CRAWFORD+ TOF LINAC CFD OPTMDL GRPH
CE		TOTAL XSECT	EXPT-PROG	7.0 5	9.0 6	UKNDC	P63	62	7/74	GLS	CRAWFORD+ TOF LINAC CFD OPTMDL GRPH
PR		TOTAL XSECT	EXPT-PROG	7.0 5	9.0 6	UKNDC	P63	62	7/74	GLS	CRAWFORD+ TOF LINAC CFD OPTMDL GRPH
ND		TOTAL XSECT	EXPT-PROG	7.0 5	9.0 6	UKNDC	P63	62	7/74	GLS	CRAWFORD+ TOF LINAC CFD OPTMDL GRPH
SM		TOTAL XSECT	EXPT-PROG	7.0 5	9.0 6	UKNDC	P63	62	7/74	GLS	CRAWFORD+ TOF LINAC CFD OPTMDL GRPH
SM	149	EVALUATION	EVAL-PROG			UKNDC	P63	55	7/74	WIN	STORY+ TBC
GD		TOTAL XSECT	EXPT-PROG	7.0 5	9.0 6	UKNDC	P63	62	7/74	GLS	CRAWFORD+ TOF LINAC CFD OPTMDL GRPH
GD	155	EVALUATION	EVAL-PROG			UKNDC	P63	55	7/74	WIN	STORY+ TBC
GD	157	EVALUATION	EVAL-PROG			UKNDC	P63	55	7/74	WIN	STORY+ TBC
DY		TOTAL XSECT	EXPT-PROG			UKNDC	P63	62	7/74	GLS	CRAWFORD+ TOF LINAC CFD OPTMDL GRPH
HO		TOTAL XSECT	EXPT-PROG			UKNDC	P63	62	7/74	GLS	CRAWFORD+ TOF LINAC CFD OPTMDL GRPH
ER		TOTAL XSECT	EXPT-PROG			UKNDC	P63	62	7/74	GLS	CRAWFORD+ TOF LINAC CFD OPTMDL GRPH
YB		TOTAL XSECT	EXPT-PROG			UKNDC	P63	62	7/74	GLS	CRAWFORD+ TOF LINAC CFD OPTMDL GRPH
HF		TOTAL XSECT	EXPT-PROG	7.0-2	1.0 4	UKNDC	P63	11	7/74	HAR	MOXON+ TOF LINAC 8 SAMPLES GRPH
HF		TOTAL XSECT	EXPT-PROG	2.0 2	1.0 5	UKNDC	P63	17	7/74	HAR	UTTLEY+ TOF LINAC OKS MOXON <2.5 KEV
HF		N,GAMMA	EXPT-PROG	7.0-3	1.0 5	UKNDC	P63	11	7/74	HAR	MOXON+ TOF LINAC RESON ANAL TBC GRAPH

Element S	A	Quantity	Type	Energy Min.	Max.	Documentation Ref.	Vol.	Page	Date	Lab.	Comments
HF	174	RESON PARAMS	EXPT-PROG	1.3 1	3.0 1	UKNDC	P63	11	7/74	HAR	MOXON+ WN FROM TRANS CAPT DATA TBC
HF	176	TOTAL XSECT	EXPT-PROG	7.0-2	1.0-4	UKNDC	P63	11	7/74	HAR	MOXON+ TOF LINAC
HF	176	RESON PARAMS	EXPT-PROG	8.0 0	2.6 2	UKNDC	P63	11	7/74	HAR	MOXON+ WN FROM TRANS+CAPT DATA TBC
HF	176	N,GAMMA	EXPT-PROG	7.0-3	1.0 5	UKNDC	P63	11	7/74	HAR	MOXON+ TOF LINAC
HF	177	TOTAL XSECT	EXPT-PROG	7.0-2	1.0 4	UKNDC	P63	11	7/74	HAR	MOXON+ TOF LINAC
HF	177	RESON PARAMS	EXPT-PROG	1.1 0	3.3 1	UKNDC	P63	11	7/74	HAR	MOXON+ WG WN FROM TRANS+CAPT DATA
HF	177	N,GAMMA	EXPT-PROG	7.0-3	1.0 5	UKNDC	P63	11	7/74	HAR	MOXON+ TOF LINAC
HF	178	TOTAL XSECT	EXPT-PROG	7.0-2	1.0 4	UKNDC	P63	11	7/74	HAR	MOXON+ TOF LINAC
HF	178	RESON PARAMS	EXPT-PROG	7.8 0	2.1 3	UKNDC	P63	11	7/74	HAR	MOXON+ WN FROM TRANS+CAPT DATA TBC
HF	178	N,GAMMA	EXPT-PROG	7.0-3	1.0 5	UKNDC	P63	11	7/74	HAR	MOXON+ TOF LINAC
HF	179	TOTAL XSECT	EXPT-PROG	7.0-2	1.0 4	UKNDC	P63	11	7/74	HAR	MOXON+ TOF LINAC
HF	179	RESON PARAMS	EXPT-PROG	5.7 0	3.1 1	UKNDC	P63	11	7/74	HAR	MOXON+ WG WN FROM TRANS+CAPT DATA
HF	179	N,GAMMA	EXPT-PROG	7.0-3	1.0 5	UKNDC	P63	11	7/74	HAR	MOXON+ TOF LINAC
HF	180	TOTAL XSECT	EXPT-PROG	7.0-2	1.0 4	UKNDC	P63	11	7/74	HAR	MOXON+ TOF LINAC
HF	180	RESON PARAMS	EXPT-PROG	7.3 1	1.1 4	UKNDC	P63	11	7/74	HAR	MOXON+ WN FROM TRANS+CAPT DATA TBC
HF	180	N,GAMMA	EXPT-PROG	7.0-3	1.0 5	UKNDC	P63	11	7/74	HAR	MOXON+ TOF LINAC
AU	197	EVALUATION	EVAL-PROG			UKNDC	P63	55	7/74	HAR	STORY+ TBC
TH	232	FISS YIELD	EVAL-PROG			UKNDC	P63	59	7/74	HAR	CROUCH EVAL OF INDEPENDENT YLD TBC
U	233	FISS YIELD	EVAL-PROG			UKNDC	P63	59	7/74	HAR	CROUCH EVAL OF INDEPENDENT YLD TBC
U	234	FISSION	EXPT-PROG			UKNDC	P63	39	7/74	ORL	JAMES+ TOF LINAC MEDT IN WF
U	235	FISSION	EVAL-PROG	1.0 2	2.0 7	UKNDC	P63	46	7/74	HAR	SOWERBY+ LINKED EVAL UPDATED TBP
U	235	FISSION	EXPT-PROG	1.0 4	4.0 4	UKNDC	P63	38	7/74	ORL	JAMES+ ANAL FOR INTERMEDIATE STRUCT
U	235	ALPHA	EXPT-PROG	FAST		UKNDC	P63	57	7/74	HAR	CROUCH+ INTEGRAL MEAS DFR TBC
U	235	SPEC FISS N	EXPT-PROG	5.1 5		UKNDC	P63	10	7/74	HAR	ADAMS+ TOF VDG JOINT EXPT SWR TBC
U	235	SPEC FISS N	EXPT-PROG	2.0 5	2.0 6	UKNDC	P63	26	7/74	HAR	NAIR+ TOF LINAC ANG DIST FISS N TBC
U	235	FISS YIELD	EXPT-PROG	FAST		UKNDC	P63	57	7/74	HAR	CROUCH+ MASS SPEC MEAS DFR TBC 1974
U	235	FISS YIELD	EXPT-PROG	1.3 5	1.7 6	UKNDC	P63	57	7/74	HAR	CUNINGHAME+ YLD MO-99 BA-140 ND-147
U	235	FISS YIELD	EXPT-PROG	FAST		UKNDC	P63	57	7/74	HAR	CUNINGHAME+ YLDS IN DIFF ZEBRA SPEC

Element S	A	Quantity	Type	Energy Min.	Max.	Documentation Ref.	Vol.	Page	Date	Lab.	Comments
U	235	FISS YIELD	EVAL-PROG			UKNDC	P63	59	7/74	HAR	CROUCH EVAL OF INDEPENDENT YLD TBC
U	235	FISS YIELD	EXPT-PROG	FAST		UKNDC	P63	58	7/74	DOU	SINCLAIR+ MASS SPEC MEAS DFR PFR TBC
U	235	N,GAMMA	EXPT-PROG	1.0 4	4.0 4	UKNDC	P63	38	7/74	ORL	JAMES+ ANAL FOR INTERMEDIATE STRUCT
U	238	RESON PARAMS	EXPT-PROG		1. 5	UKNDC	P63	25	7/74	HAR	SOWERBY+ EXPT TO TEST RES PARAMS TBD
U	238	TOTAL INELST	THEO-PROG		3. 6	UKNDC	P63	46	7/74	HAR	LYNN SIG FOR (N,GN') GRPH
U	238	FISSION	EXPT-PROG	4.0 5	2.2 7	UKNDC	P63	35	7/74	HAR	COATES+ TOF CYCLOTRON REL U-235 GRPH
U	238	FISSION	EVAL-PROG	6.0 5	2.0 7	UKNDC	P63	46	7/74	HAR	SOWERBY+ LINKED EVAL UPDATED TBP
U	238	SPEC FISS N	EXPT-PROG	1.3 6	2.3 6	UKNDC	P63	26	7/74	HAR	NAIR+ TOF LINAC ANG DIST FISS N TBC
U	238	F NEUT DELAY	EVAL-PROG			UKNDC	P63	55	7/74	WIN	SMITH EVAL OF TOMLINSON REVISED
U	238	ALPHA	EXPT-PROG	FAST		UKNDC	P63	57	7/74	HAR	CROUCH+ INTEGRAL MEAS DFR TBC
U	238	FISS YIELD	EXPT-PROG	FAST		UKNDC	P63	57	7/74	HAR	CROUCH+ MASS SPEC MEAS DFR TBC
U	238	FISS YIELD	EXPT-PROG	FAST		UKNDC	P63	57	7/74	HAR	CUNINGHAME+ YLDS IN DIFF ZEBRA SPEC
U	238	FISS YIELD	EVAL-PROG			UKNDC	P63	59	7/74	HAR	CROUCH EVAL OF INDEPENDENT YLD TBC
U	238	N,GAMMA	EVAL-PROG	1.0 3	2.0 7	UKNDC	P63	46	7/74	HAR	SOWERBY+ LINKED EVAL UPDATED TBP
NP	237	HALF LIFE	EXPT-PROG			UKNDC	P63	58	7/74	HAR	GLOVER+ TBC
PU	239	FISSION	EVAL-PROG	1.0 2	2.0 7	UKNDC	P63	46	7/74	HAR	SOWERBY+ LINKED EVAL UPDATED TBP
PU	239	ALPHA	EXPT-PROG	FAST		UKNDC	P63	57	7/74	HAR	CROUCH+ INTEGRAL MEAS DFR TBC
PU	239	F NEUT DELAY	EVAL-PROG			UKNDC	P63	55	7/74	WIN	SMITH EVAL OF TOMLINSON REVISED
PU	239	FISS YIELD	EXPT-PROG	1.3 5	1.7 6	UKNDC	P63	57	7/74	HAR	CUNINGHAME+ VDG YLD VS EN TBD
PU	239	FISS YIELD	EXPT-PROG	FAST		UKNDC	P63	57	7/74	HAR	CUNINGHAME+ YLDS IN DIFF ZEBRA SPEC
PU	239	FISS YIELD	EXPT-PROG	FAST		UKNDC	P63	57	7/74	HAR	CROUCH+ MASS SPEC MEAS DFR TBC
PU	239	FISS YIELD	EXPT-PROG	FAST		UKNDC	P63	58	7/74	DOU	SINCLAIR+ MASS SPEC MEAS DFR PFR TBC
PU	239	FISS YIELD	EVAL-PROG			UKNDC	P63	59	7/74	HAR	CROUCH EVAL OF INDEPENDENT YLD TBC
PU	239	HALF LIFE	EXPT-PROG			UKNDC	P63	58	7/74	HAR	GLOVER+ TBC
PU	240	FISS YIELD	EXPT-PROG	FAST		UKNDC	P63	58	7/74	DOU	SINCLAIR+ MASS SPEC MEAS DFR PFR TBC
PU	240	FISS YIELD	EVAL-PROG			UKNDC	P63	59	7/74	HAR	CROUCH EVAL OF INDEPENDENT YLD TBC
PU	241	FISS YIELD	EVAL-PROG			UKNDC	P63	59	7/74	HAR	CROUCH EVAL OF INDEPENDENT YLD TBC
PU	242	F NEUT DELAY	EVAL-PROG			UKNDC	P63	55	7/74	WIN	SMITH EVAL OF TOMLINSON REVISED

Element S	A	Quantity	Type	Energy Min.	Max.	Documentation Ref.	Vol.	Page	Date	Lab.	Comments
AM	243	N,GAMMA	EXPT-PROG	FAST		UKNDC	P63	58	7/74	HAR	GLOVER PROD SIG CM-244 IN ZEBRA TBD
CF	252	NU	EXPT-PROG	SPON		UKNDC	P63	61	7/74	NPL	AXTON EVAL MN BATH CORR TBC
H2O		THRMLSCAT LAW	EVAL-PROG			UKNDC	P63	55	7/74	WIN	BUTLAND NEW DATA AT 7 TEMPS
D2O		THRMLSCAT LAW	EVAL-PROG			UKNDC	P63	55	7/74	WIN	BUTLAND NEW DATA AT 7 TEMPS
MANY		EVALUATION	EVAL-PROG	3.0 6	1.4 7	UKNDC	P63	50	7/74	HAR	FERGUSON COMMON STRUCTURAL MATERIALS
MANY		FISS YIELD	EVAL-PROG	FAST		UKNDC	P63	59	7/74	HAR	CROUCH OBJECTIVE EVAL UPDATES R-7394
MANY		FISS PROD G	EVAL-PROG			UKNDC	P63	59	7/74	UK	TOBIAS BETA-GAMMA DECAY SCHS ALL FP
MANY		ALPHA ES	EVAL-PROG			UKNDC	P63	59	7/74	HAR	ROGERS ALPHA ES AND INTENS TBC

CONTENTS

TABLES

ILLUSTRATIONS

ILLUSTRATIONS
(Cont'd.)

NUCLEAR PHYSICS DIVISION, A.E.R.E. HARWELL

(Division Head: Dr. B. Rose)

Editorial Note

Since the results obtained from the various machines are not easily classified according to the energy of the charged beams, individual research items are labelled with a single letter indicating on which machine the experiments were performed. These labels are as follows:

A. 3 MV pulsed Van de Graaff IBIS (A.T.G. Ferguson)

B. 45 MeV Electron Linac (J.E. Lynn)

C. Synchrocyclotron (A.E. Taylor and C. Whitehead)

D. 14 MeV Tandem Generator (J.M. Freeman)

A. Measurement of the ^{235}U Fast Neutron Fission Spectrum (J.M. Adams and P.I. Johansson (Studsvik)) [Relevant to Request numbers: 691256, 691257, 692376, 721080, 742077]

This collaborative measurement, using IBIS, the Harwell 3 MeV pulsed Van de Graaff, arose as a result of differences in the previous ones conducted independently at Harwell(1) and at Studsvik (P.I. Johansson et al)(2).

The ^{235}U fast neutron fission spectrum has been measured at an incident neutron energy of 0.51 MeV and at a lab. angle of 90°. The fast neutron scintillation detector comprised a 11.4 cm diam. by 5 cm thick NE213* (bubble-free) scintillator coupled to a 12.7 cm RCA 8854 photomultiplier+ and utilised the Harwell n-γ pulse shape discrimination system. All measurements were conducted at a flight path of 3 metres, and the primary neutrons were generated by the $^{7}Li(p,n)^{7}Be$ reaction using a Li metal target. The neutron detector was specially constructed for this work and its neutron efficiency has also been measured. The calibration of the energy scale of the fission spectrum was obtained using neutrons from the $^{10}B(d,n)^{11}C$ and $^{11}B(d,n)^{12}C$ reactions, giving an empirical calibration up to ~16 MeV, whereas the previous independent Harwell and Studsvik measurements had empirical calibrations extending to at most 9 MeV. It has been established that it is the energy calibration that is by far the most crucial aspect in the analysis of the fission spectrum.

At the present time the analysis of the data is in progress. However a preliminary analysis has been carried out using the Studsvik curve for the efficiency of the neutron detector. These preliminary results indicate a spectrum lying between those previously obtained at Harwell and Studsvik and give the following fits to a Maxwellian shape ($N(E) = C\sqrt{E}\, e^{-E/T}$).

(i) Up to 7-8 MeV T = 1.35-1.38 MeV
(ii) Up to 15 MeV T = 1.46 MeV (poor fit).

These results can be compared with the previous data: Studsvik obtained a value for T of 1.29 MeV for a Maxwellian shape for neutron energies up to 13-14 MeV while a significant departure from a Maxwellian shape was observed above ~7 MeV in the Harwell measurement. For the joint Harwell Studsvik data there is good experimental evidence for a neutron excess at higher neutron energies compared with a Maxwellian shape, unlike the Studsvik data, but the deviation is less than that of the earlier Harwell data. However more analysis is required to quantify this more precisely.

In the absence, initially, of a complete efficiency curve for the neutron detector used, it seemed reasonable to use the Studsvik efficiency curve since the scintillators were similar (viz. Studsvik 12.7 cm diam. by 5 cm thick coupled to a 5 cm RCA 8850 photomultiplier)+, and the biases were the same. However the PSD systems differ which

---

*Supplied by Nuclear Enterprises (G.B.) Ltd.

+Supplied by RCA.

(1) UKNDC(73)P53, EANDC(UK)151L, INDC(UK)-20L.

(2) P.I. Johansson, private communication.

may well affect the lower neutron energies. Normalisation of the Harwell/Studsvik data to the Studsvik data indicates an unphysical efficiency for this work above ~8 MeV. Also there is a difference in the efficiency curve 'shapes' at lower neutron energies, which may well be sufficient to alter the Maxwellian fit. The efficiency curve for the Harwell data could not be used since the bias was lower (viz. 1/10 Am bias), and the scintillator was much smaller, (viz. 5 cm diam. by 3.8 cm thick, coupled to a 5 cm RCA 8850 photomultiplier).

B. Measurements of the neutron cross-sections of natural hafnium and its stable isotopes (M.C. Moxon, J.E. Jolly and D.A.J. Endacott) [Relevant to Request Numbers: 621023, 621024, 621026, 732088, 621028, 692032, 621030, 621032, 692035, 671080, 692034, 732089]

Measurements of the total cross-section and capture cross-section of natural hafnium have been carried out on the Harwell 45 MeV electron linac neutron time-of-flight facility. Total and capture cross-section measurements are also being carried out on samples enriched in each of ^{176}Hf, ^{177}Hf, ^{178}Hf, ^{179}Hf and ^{180}Hf on loan from the USAEC.

The total cross-section of the natural element was measured using transmission techniques on a 14 m flight path on the neutron booster target of the linac. Transmission measurements were carried out on up to 8 sample thicknesses of metallic hafnium. The overall neutron energy range is ~0.07 eV to ~10 keV and measurements in each energy range were carried out on at least two samples varying in thickness by at least a factor of two. Figure 1 shows an example of the transmission data for the 1 cm sample of natural Hf.

As area analysis of the resonance data can only be used on isolated resonances and as at least half the resonances in natural hafnium are too close to allow accurate estimates of the integrated transmission dip (area) due to single levels to be made, we had to use detailed shape fitting techniques of resonance analysis. Examples of multi-sample shape fitting are shown in the report on the analysis of neutron transmission data (M.C. Moxon, this report, p.17). It was virtually impossible to carry out simple area analysis on the resonances at 5.7 and 5.9 eV even for the data from the thinnest sample.

Analysis of the data in terms of resonance parameters is almost complete up to 20 eV and it is thought that only minor adjustments due to alteration of resonance parameters outside this range will be necessary. However, recent examination of capture measurements on a sample enriched in ^{176}Hf indicate a resonance in the cross-section of this isotope at ~7.93 eV with a neutron width of 10–20 meV and a radiation width of ~50 meV. A resonance with parameters similar to these would explain the value of the resonance integral (given as 700±50 b in BNL 325). Measurement of capture gamma spectra by T. Haste on the ^{176}Hf sample confirmed the presence of capture due to ^{176}Hf in the region around 7.9 eV. A resonance of this size would be obscured in measurements on natural samples by the large resonance in the cross-section of ^{178}Hf at 7.83 eV.

Between 20 and 40 eV analysis of the data on natural hafnium is reasonably complete. Owing to the overlap of resonances in different isotopes, the analysis of the data on the separated isotopes may affect the distribution of the parameters in a given group of resonances but not the total area of the group. Only preliminary analysis has been carried out on the data above 40 eV.

Figure 2 shows the measured total cross-section below 10 eV and the curve calculated from the resonance parameters obtained from fits to multi-sample data, which employ the assumption that the peak at 7.83 eV is entirely due to the resonance in ^{178}Hf.

Capture cross-section measurements have been carried out on metallic samples of natural hafnium and one sample of each of the enriched isotopes at the 4 m flight path station on the plain uranium target of the linac and at the 32 m station on the neutron booster target of the linac. The 4 m capture data extends over a neutron energy range of ~0.007 eV to ~100 eV and the 32 m data from ~5 eV to ~100 keV.

The total and capture cross-section of natural hafnium below 0.8 eV are shown in Figure 3. The thermal capture cross-section (at neutron energy 0.0253 eV) determined from the data is 103±2 b and is in reasonable agreement with other types of measurements. The preliminary analysis of the data gives thermal capture cross-sections in agreement with values given in BNL 325. A thermal capture cross-section of ~2500 b is obtained for ^{174}Hf using the isotope data in conjunction with the measurements on samples of natural hafnium. This value is a factor ~6 higher than the value quoted in BNL 325 and is as yet unexplained. The average capture cross-section of natural hafnium in the neutron energy region 1 to 100 keV is shown in Figure 4. These data are in reasonable agreement with those of Block et al[(1)] but are about a factor of two above the data of Macklin et al[(2)] at 30 and 60 keV.

The analysis of the resonances from the data measured at the 4 m and 32 m capture detectors is being carried out using shape fitting programmes incorporating a Monte Carlo technique to correct for multiple scattering effects. Initial parameters obtained from the capture data are in good agreement with the parameters given by the transmission data.

---

(1) R.C. Block, G.G. Slaughter, L.W. Weston and F.C. Vondar Lage, Neutron Time of Flight Methods Conference, Saclay (1961) p.203.

(2) R.L. Macklin, J.H. Gibbons and T. Inada, Phys. Rev. 129 (1963) 2695.

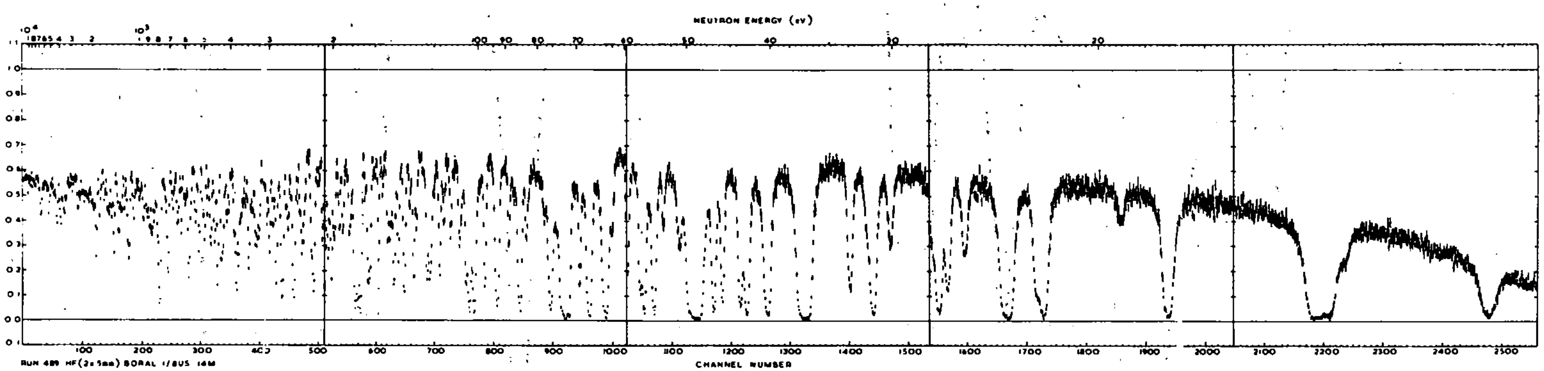

Fig. 1 Measurement of the neutron transmission through a 1 cm thick sample of natural hafnium

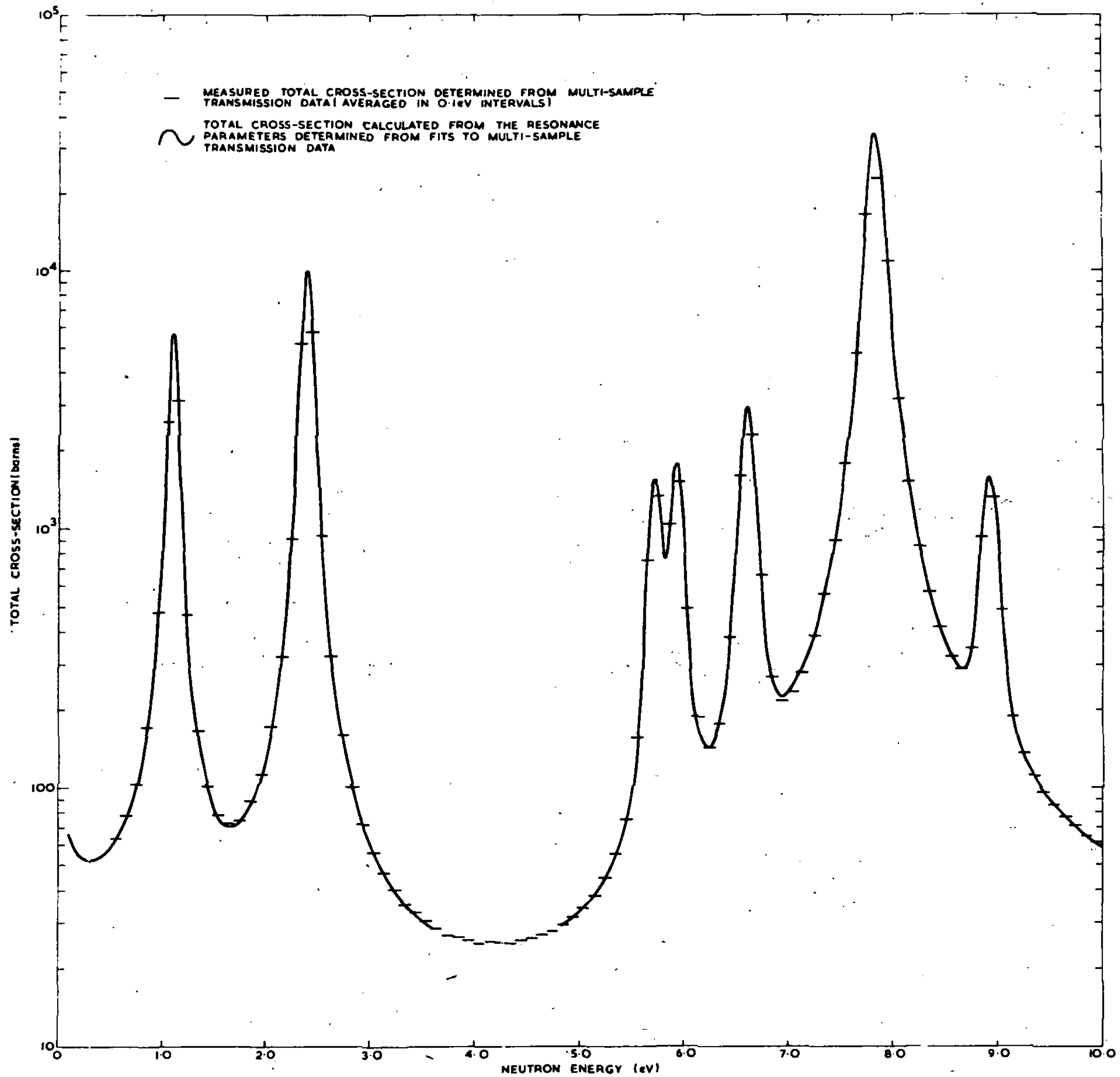

Fig. 2 Total cross-section of natural hafnium below 10 eV showing the experimental data together with a curve calculated from resonance parameters derived from the transmission data

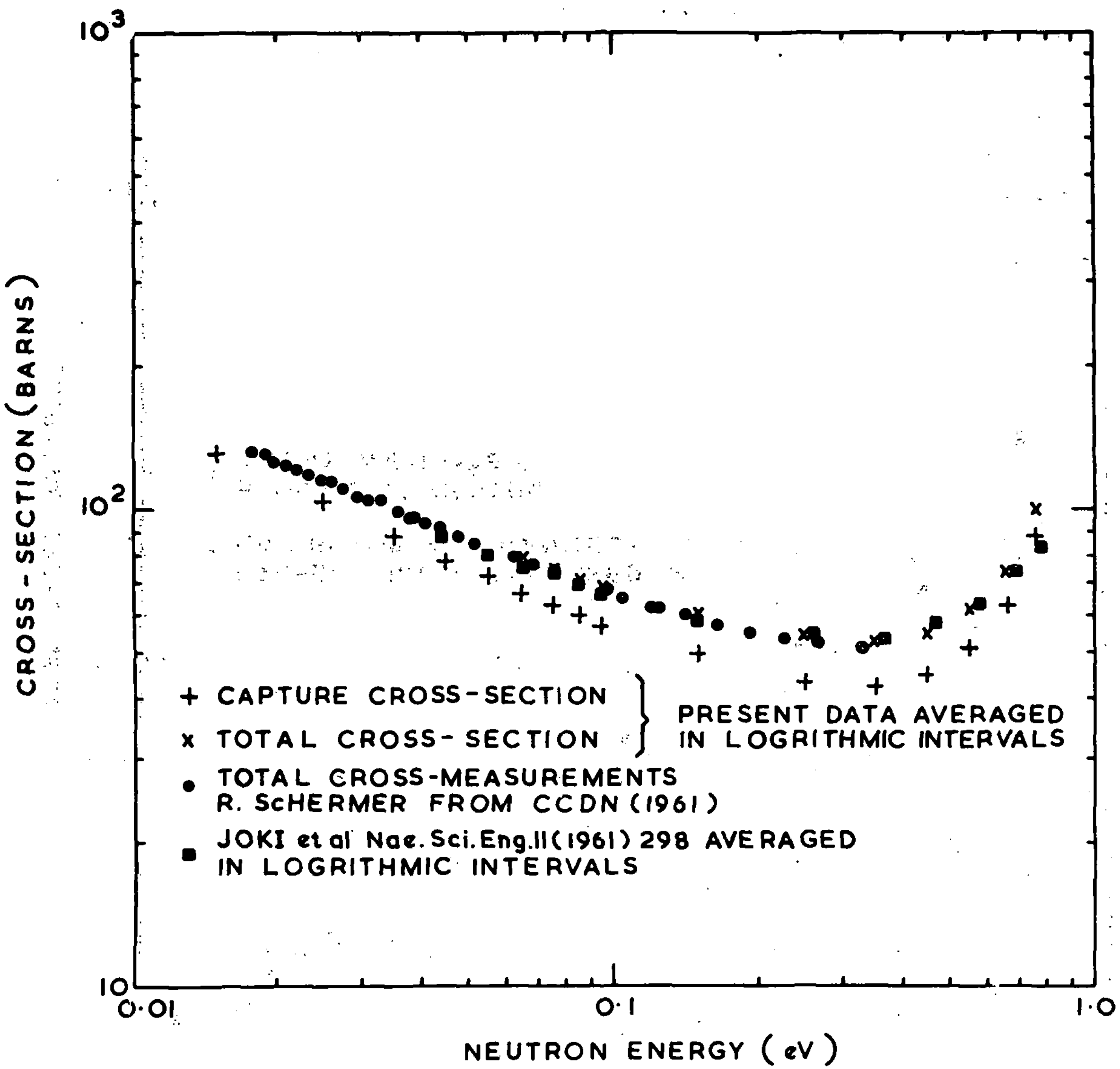

Fig. 3 The total and capture cross-sections of natural hafnium between ~0.01 and 0.8 eV

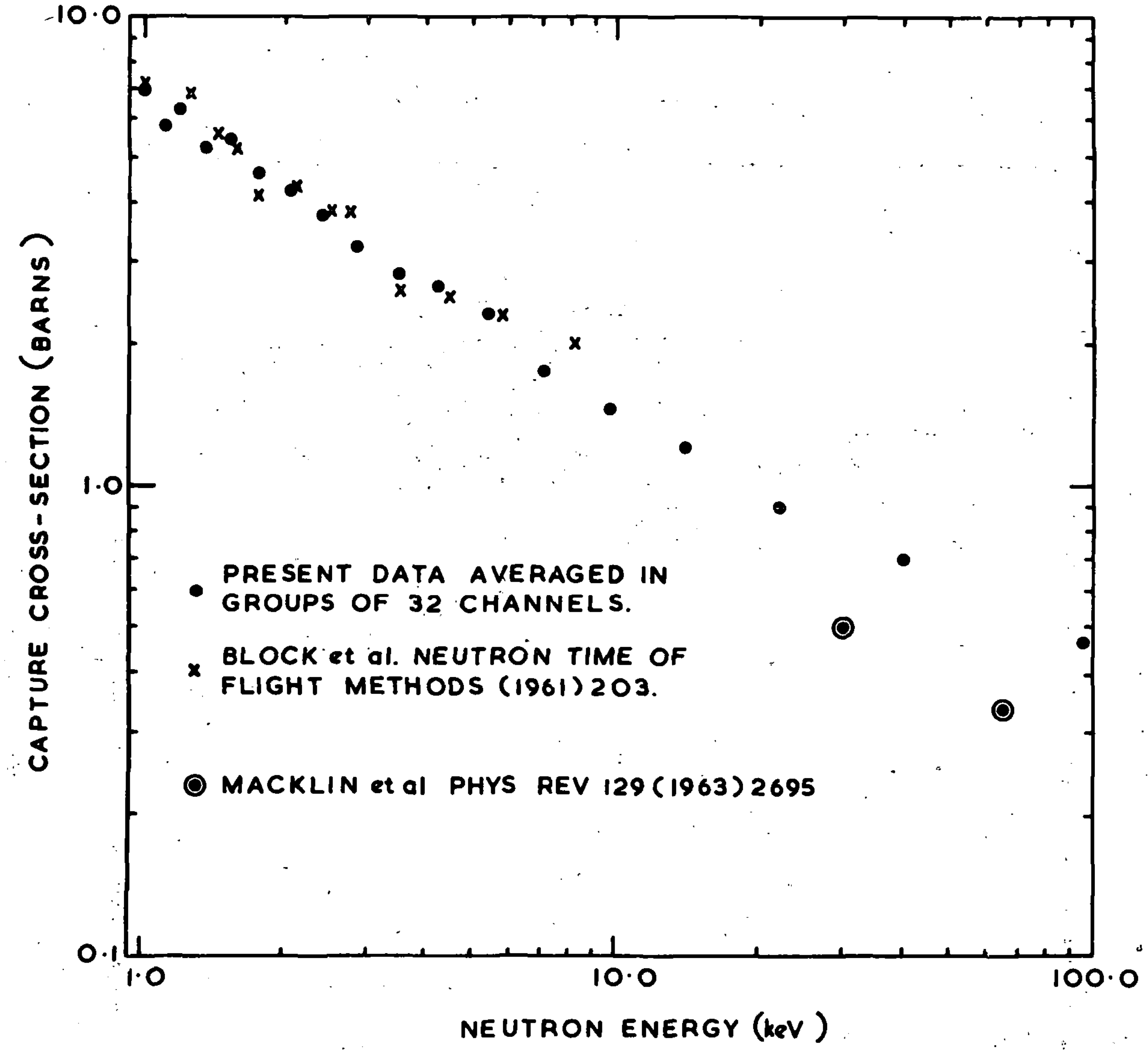

Fig. 4 The average capture cross-section of natural hafnium in the neutron energy range 1 to 100 keV

B. Total cross-section of natural hafnium (C.A. Uttley and M.S. Coates)

The transmission of three samples of natural hafnium of thicknesses 4.24×10^{-3}, 2.083×10^{-2} and 4.1896×10^{-2} at/b have been measured using the 120 m and 60 m spectrometers on the 45 MeV linac. The detector at 120 m consisted of a ^{10}B plus vaseline mixture surrounded by four NaI(Tl) crystals and photomultipliers. The detector at the intermediate station at 60 m on the same flight path comprised the ^{10}B powder overlap filter, serving the 120 m spectrometer, surrounded by three NaI(Tl) crystals and phototubes.

The samples were cycled in and out of the beam at 60 m at which point was placed a permanent Manganese filter to monitor the background from both the detectors. In some runs a Cobalt black resonance filter was also used. The energy range of the measurements was from 20 eV to 0.1 MeV using the 60 m data for the resonance region below 2.5 keV and the 120 m data for the remainder. Thus a permanent filter of sulphur was used in front of the 120 m detector to monitor the background just above 0.1 MeV.

A 16 track 8 MHz tape recorder was used in which two bits coded the position of the sample changer and the detector from which the stop pulses were received, and 13 bits gave time-of-flight information. Measurements of the carbon total cross-section were made before and during the hafnium runs as a check on the absolute accuracy of the equipment and background determinations. The resonance data from 60 m are in agreement with those of Moxon et al. (this report, p.11) and the 120 m data are being processed.

The analysis of neutron transmission data (M.C. Moxon)

There has long been the requirement for a general computer programme to determine neutron resonance parameters from neutron time-of-flight data by a detailed "shape" fitting procedure. This is especially true in the case of multi-isotope elements and for isotopes with a small level spacing, where area analysis (which can only treat isolated resonances) cannot be used because of the close proximity of the resonances.

A Fortran programme based on the Harwell library(1) routine VA02A for minimisation of multi-variable functions has been developed to carry out a least squares fit to neutron transmission data. It uses the generalised multi-level R-matrix formalism for the nuclear cross-section. The effect of Döppler broadening is calculated from the classical gas model with an adjustable effective temperature to take into account solid-state quantal effects. The transmission due to the Döppler broadened cross-section is calculated and the resolution function is folded in before comparison with the observed data is carried out.

The programme at present can perform simultaneous fits on up to 20 runs of different sample thickness and resolution. In using the program in the multi-sample mode it soon becomes apparent that other parameters as well as the resonance parameters have to be adjusted.

The energy scale is fixed using one of the runs and a time shift at the origin of the time-of-flight scale is adjusted for the other runs. In most cases this is less than one time-channel width. The data on each run are given a re-normalising parameter;

---

(1) M.J. Hopper, AERE - R 7477 (1973).

this allows for errors in monitoring and it is also necessary because the parameters used for some of the nearby resonances and/or the potential scattering length may be in error. The adjustment to the potential scattering length is best carried out, using the data in the regions between the resonances, after determination of the resonance parameters. The use of very thick samples that gave zero transmission at several resonances revealed a possible small over determination of the background. This is probably due to inclusion of some of the long tail on the resolution function in the background data. The resolution parameters can also be adjusted, such as the slowing down path length or target decay time.

A simultaneous multi-sample fit to the data in the region of the 2.4 eV resonance in natural hafnium summarised in Table 1 is shown in Figure 5. The neutron width is in good agreement with that obtained from area analysis on the thinnest samples. Area analysis could not be carried out on the thicker samples, due to interference of nearby resonances. Accurate area analysis was impossible, even on the thinnest samples, for the 5.7 and 5.9 eV resonances in natural hafnium and Figure 6 shows the fit to the data summarised in Table 2 in the region of these resonances. Even using the fitting programme, the thicker samples did not improve the accuracy of the parameters given by the three thinnest ones.

Care should be taken in interpreting the significance of the values of χ^2 given in Tables 1 and 2 because the effect of systematic errors may have been overestimated in the present analysis.

The main problem with this fitting programme at present is that it requires ~800 K bytes of fast computer store and 1500 K bytes of disc storage space.

TABLE 1

Least-square fit to the neutron transmission data in the region of the 2.4 eV resonance in hafnium

Run Number	Sample Thickness atoms/b	Initial zero time μsec	Original channel width μsec	No. of channels summed	Adjusted zero time μsec	Adjusted Normalisation	Adjusted Background	χ^2	No. of data points
466	0.8548×10^{-4}	8.209	0.5	5	Standard	1.026	–	39	60
470	0.8548×10^{-4}	8.309	0.5	5	8.314	1.019	–	27	60
523	0.1763×10^{-3}	8.309	0.5	5	8.311	1.012	–	47	28
525	0.1763×10^{-3}	8.309	0.5	5	8.307	1.001	0.00375	32	28
478	0.3419×10^{-3}	8.059	0.5	5	8.063	0.992	–	96	63
517	0.3419×10^{-3}	8.309	0.5	5	8.310	1.001	–	37	42
520	0.3419×10^{-3}	8.309	0.5	5	8.307	1.001	-0.00306	40	42
509	0.4130×10^{-2}	8.309	0.5	10	8.310	0.999	–	32	38
506	0.1080×10^{-1}	8.209	0.5	10	8.211	1.000	–	10	50
507	0.1080×10^{-1}	8.209	0.5	10	8.208	1.001	–	18	50
494	0.2119×10^{-1}	8.309	0.5	5	8.299	0.994	–	35	68
495	0.2119×10^{-1}	8.209	0.5	10	8.217	0.983	-0.00373	33	60
496	0.4208×10^{-1}	8.309	0.5	10	8.313	0.999	-0.00047	8	60
497	0.4208×10^{-1}	8.109	0.5	10	8.103	0.983	0.00089	42	60

Resonance energy = 2.4027 eV
Neutron width = 8.132 meV
Radiation width = 61.74 meV
Total chi-squared = 495.6
Total number of points = 709
No. of fitted parameters = 35
χ^2 per degree of freedom = 0.735

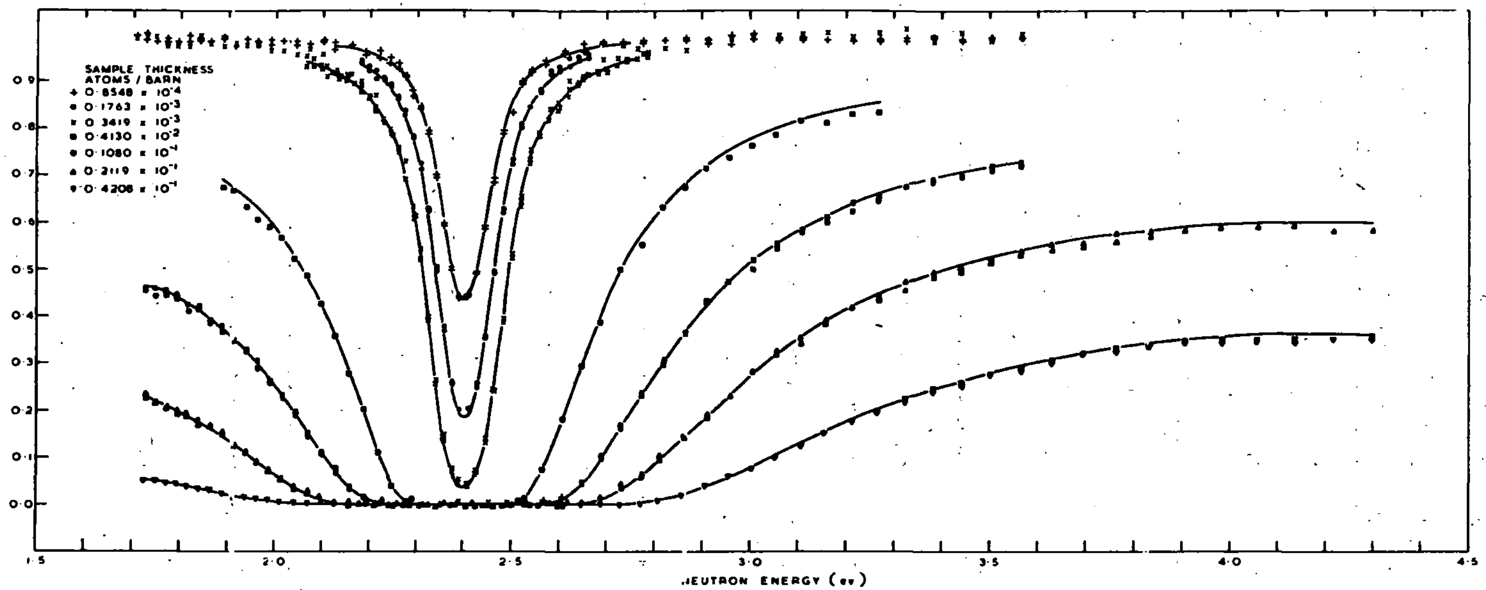

Fig. 5 Least-square fit to the neutron transmission data in the region of the 2.4 eV resonance in hafnium

TABLE 2

Least-square fit to the neutron transmission data in the region of the 5.7 and 5.9 eV resonances in hafnium

Run Number	Sample Thickness atoms/b	Initial zero time μsec	Original channel width μsec	No. of channels summed	Adjusted zero time μsec	Adjusted Normalisation	Adjusted Background	χ^2	No. of data points
466	0.8548×10^{-4}	8.309	0.5	1	Standard	1.023	–	44	51
470	0.8543×10^{-4}	8.370	0.5	1	8.109	1.019	–	53	51
523	0.1763×10^{-3}	8.368	0.5	1	8.154	1.007	–	70	61
478	0.3419×10^{-3}	8.228	0.5	1	8.212	1.002	–	55	61
517	0.3419×10^{-3}	8.292	0.5	1	8.175	1.012	–	53	61

Resonance energy	=	5.9378 eV	5.7292 eV
Neutron width	=	5.226 meV	4.318 meV
Radiation width	=	62.54 meV	54.80 meV
Total chi-squared	=	274	
Total no. of points	=	285	
No. of fitted parameters	=	15	
χ^2 per degree of freedom	=	1.02	

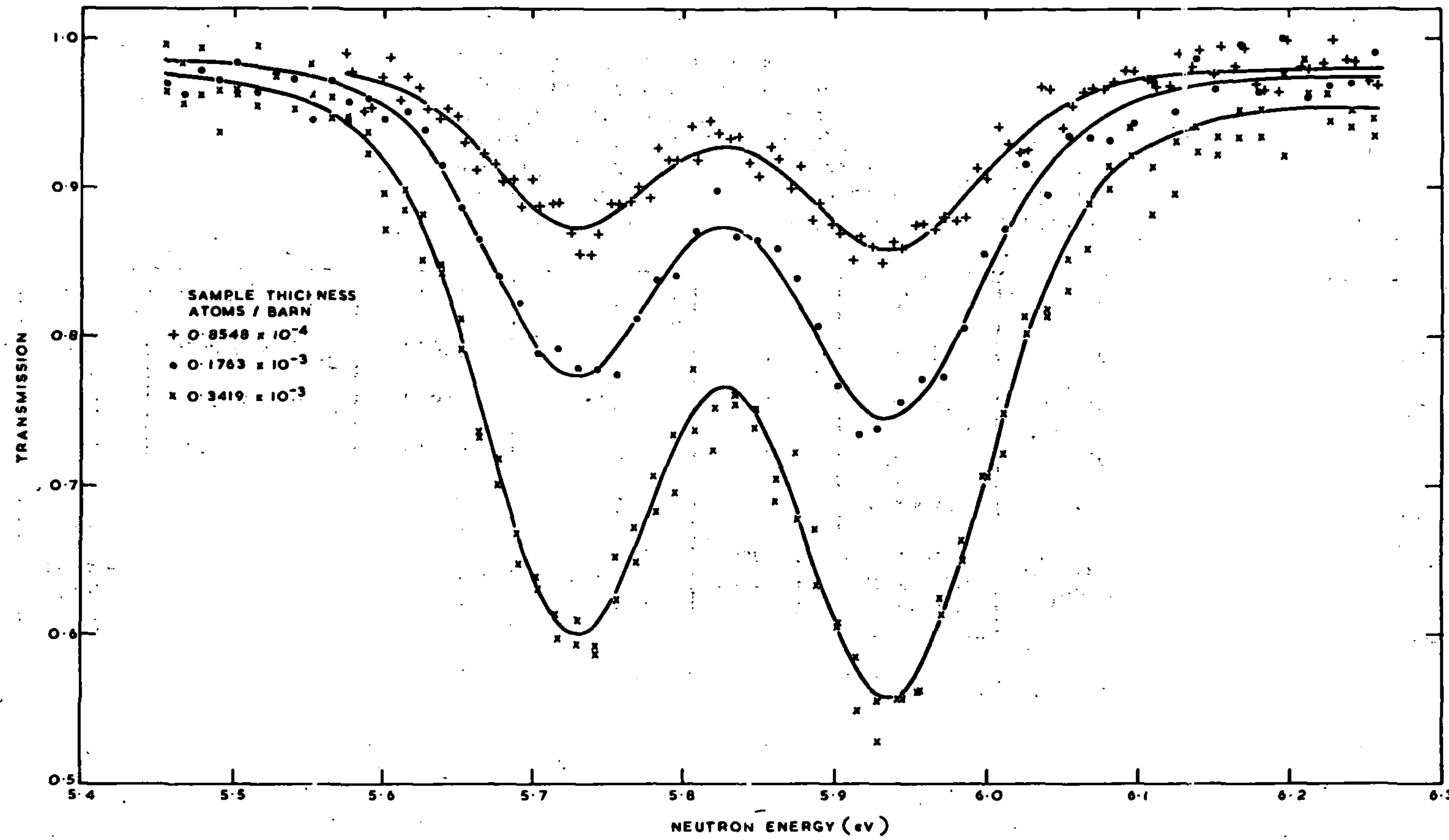

Fig. 6 Least-square fit to the neutron transmission data in the region of the 5.7 and 5.9 eV resonances in hafnium

B. Energy calibration on the Linac (C.A. Uttley and M.S. Coates)

In recent years some systematic differences in energy scale have been observed between Van de Graaff accelerators and the Harwell Linac on cross-sections which are of general interest and suitable as neutron standards. The discrepancies are observed only at energies below a few hundred keV where the linac energy resolution is better than that normally achieved by the Van de Graaff. Typically the energy difference is ~5 keV at 0.25 MeV but this difference persists down to the lowest energy usually measured by the Van de Graaff. Differences in energy of this order have been observed on the neutron total and (n,α) cross-sections of ^6Li, which peak near 0.25 MeV, and systematic increases in the carbon total cross-section over that measured on the linac near 0.1 MeV have been attributed to the linac energy scale being invariably lower than the Van de Graaff.

In an attempt to resolve the discrepancies and to compare the linac energy calibration with the Columbia and Karlsruhe time-of-flight spectrometers, two resonances in sodium between 0.2 and 0.3 MeV have been measured which are much narrower (by a factor of at least 25) than the resonance near 0.25 MeV in ^6Li, the recent analyses of which have been largely instrumental in indicating the different energy determinations. In this measurement, using the 120 m spectrometer, the response of the transmission detector to the γ-flash is recorded along with the neutron time spectrum with the sodium sample in the beam. Thus, the timing of both the selected resonances is easily determined since each has a minimum transmission in one time channel.

The energy of the peak cross-section of the relatively isolated s-wave resonance near 0.3 MeV, which has a width $\approx$2 keV, is 298.8±2.3 keV in our measurement compared with 298.5±1.0 keV by the Columbia University synchrocyclotron time-of-flight system(1) and a listed value of 298.4 keV by the Karlsruhe Group. There are two resonances near 240 keV which are not resolved by our spectrometer(2). The lower one is very narrow and its transmission minimum occurs at 236.3±1.6 keV. The upper resonance, above 240 keV, is broader with a lower peak cross-section but its existence makes the second energy calibration point less satisfactory than the first for differing instrumental resolutions.

It should be pointed out in conclusion that the energy of the peak cross-section should be compared for energy calibration and not confused with resonance energies quoted from resonance analyses. The resonance energies and peak cross-sections rarely coincide for higher energy resonances owing to the increasing importance of resonance-potential scattering interference, multilevel effects and the rapid energy dependence of neutron widths for higher orbital angular momentum waves.

---

(1) S. Wynchank, INDC(USA)-39/L; EANDC(US)166L.

(2) F. Rahn, H.S. Camarda, G. Hacken, W.W. Havens, H.I. Liou, J. Rainwater, U.N. Singh, M. Slagowitz and S. Wynchank, Phys. Rev. C 8 (1973) 1827.

B. Neutron spectrum measurements using a thin ^6Li glass scintillation detector on the 100 m flight path of the neutron booster (M.S. Coates, D.B. Gayther, S. Nair (Oxford University) and B. Thom (Queen Mary College))

A 1 mm thick 6 cm dia ^6Li glass scintillation detector has been used on the 100 m flight path of the neutron booster to obtain an accurate determination of the neutron spectrum at lower energies than previously reported[1]. These earlier measurements were made with a boron-vaseline plug which had been cross calibrated against the Harwell Black Detector down to an energy of ~1 keV. The neutron detection efficiency of the present detector is known to better than ±2% below about 20 keV on the basis of present knowledge of the $^{6}Li(n,\alpha)$ cross-section[2]. The measurements were conventional with background determined by the black resonance technique. The spectrum was determined between 20 keV and 100 eV with an estimated accuracy of ~±3%. This spectrum will be used in the analysis of neutron capture cross-sections to be measured on this flight path with a large liquid scintillator (this report, p.24).

(1) D.B. Gayther, D.A. Boyce and J.B. Brisland, Nuclear Physics Division Progress Report AERE - PR/NP 19, p.1 (1972), also UKNDC(72)P37, EANDC(UK)140AL, INDC(UK)15G.

(2) C.A. Uttley, M.G. Sowerby, B.H. Patrick and E.R. Rae, Proc. of 1970 Argonne Symposium on Neutron Standards and Flux Normalisation, p.80 (1971).

A proton radiator for neutron flux measurements between 200 keV and 5 MeV

(M.S. Coates, P.A.R. Evans (Oxford University), D.B. Gayther and P.P. Thomas)

Work has started to build a proton recoil detector of the type described by Käppeler and Fröhner[1] to be used for neutron flux measurements in time-of-flight experiments over the energy region 200 keV → 5 MeV. Neutrons strike a thin film of hydrogenous material and the recoil protons are detected a few centimetres away by solid state counters lying out of the beam. At present the device is being designed in detail and it is expected to carry out practical tests within a few months. A Monte Carlo programme[2] for calibrating the detailed response of the detector to neutrons has been run successfully.

(1) F. Käppeler and F.H. Fröhner, Nuclear Data for Reactors, 1, 221, IAEA Vienna (1970).

(2) F. Käppeler, Private Communication.

B. Commissioning of a large liquid scintillator tank (M.S. Coates, D.B. Gayther and B. Thom (Queen Mary College))

Some preliminary investigations on a 270 litre liquid scintillator detector for neutron capture cross-section measurements were reported earlier[1]. It was decided to replace the central stainless steel liner tube by a beryllium sleeve instead of an aluminium one as suggested there. Other considerations prevented this change from being carried out for some time and tests indicated that the scintillator had deteriorated in the interval to such an extent that observed gamma-ray energy resolutions had worsened by a factor of 2. The tank has been refilled with new scintillator and at the same time all the photomultipliers have been replaced by ones with almost twice the cathode sensitivity. In addition a 0.05 mm sheet of aluminised Melinex has been suspended across the middle of the tank in a vertical plane to allow coincidence measurements between events occurring in the optically separated halves. It is expected that this provision will significantly reduce background rates due to cosmic ray events. Measurements of pulse height distributions obtained with ^{137}Cs, ^{60}Co and ^{24}Na gamma-ray sources show that the changes made to the system have resulted in a significant improvement in energy resolution.

(1) M.S. Coates and M.C. Moxon, Nuclear Physics Division Progress Report AERE - PR/NP 17 p6 (1970), also UKNDC(71)P28, EANDC(UK)134AL, INDC(UK)-12G.

Experiments on heated ^{238}U samples to improve the predictions of the ^{238}U Döppler temperature coefficient for fast reactors (M.G. Sowerby and D.J. Pearson (University of Wales Institute of Science and Technology)) [Relevant to Request Numbers: 691286, 692385, 702029, 714016 and 732113]

One of the largest adjustments[1] made in producing the adjusted cross-section set FGL5 was the reduction of the capture cross-section of ^{238}U by 12% below 25 keV. The integral data, which cause the reduction, relate to "thick" samples while the evaluated differential data, which had to be adjusted, come from "thin" samples. The discrepancy could therefore be due to errors in the calculation of self-screening corrections in fast reactors caused by errors in the assumed resolved and unresolved ^{238}U resonance parameters. The ^{238}U Döppler temperature coefficient for fast reactors depends critically on these parameters and therefore we have been investigating the possibility of making measurements with the linac which would test the resonance parameters and the calculation of Döppler broadening at temperatures up to 2500°K. (Integral measurements of the ^{238}U Döppler temperature coefficient for fast reactors have only been made at temperatures below ~1000°K).

So far calculations of the average transmission of U samples as a function of temperature have been made. From these it can be seen that the changes in transmission as a function of temperature are primarily due to the Döppler broadening filling in the "windows" in the total cross-section curve produced by the resonance-potential interference. These windows are large for the s-wave resonances with large Γ_n and therefore this type of measurement will test the Döppler broadening constant and the distribution of large Γ_n s-wave resonances. There is little sensitivity in the results to the values of the radiation width. Recently a start has been made on the calculation of the average self indication ratio as a function of temperature but no conclusions have been reached to date.

---

(1) J.L. Rowlands, C.J. Dean, J.D. MacDougall and R.W. Smith, Paper presented to International Symposium on Physics of Fast Reactors, Tokyo (1973).

Heating of UO_2 for Döppler broadening studies (M.S. Coates and P.P. Thomas)

The feasibility of heating samples of UO_2 to temperatures in the region of 2500°C has been investigated in a preliminary way with a view to carrying out neutron time-of-flight experiments to study Döppler broadening effects. A heating method is desired which minimises the amount of material near the sample in order that unperturbed measurements of emitted gamma-rays following neutron capture can be made. The methods of R.F. heating and ohmic heating using large currents are both far from ideal in this respect although the required temperatures can be reached. Conventional electron beam heating appeared attractive at first sight but some trial experiments using a 30 kV electron gun were unsatisfactory chiefly owing to space charge build up. At present attention is being directed to electron beam heating using a plasma gun which would overcome space charge problems and seems to offer other advantages such as increased flexibility of design and reliability in operation.

B. The angular distribution of prompt fission neutrons (S. Nair (Oxford University) and D.B. Gayther)

The existence of strongly anisotropic fission fragment angular distributions provides a means of determining the stage during the fission process at which neutron emission occurs. Thus fission neutrons emitted from the fully accelerated fragments will have an angular distribution relative to the incident beam which can be related to the fragment angular distribution, while neutrons emitted at the instant of scission are expected to be isotropic. A measurement of the prompt neutron angular distribution should therefore provide information on the fraction emitted at scission if the fragment angular distribution is already known. The large fragment anisotropies which occur in the photofission of even-mass targets provide the most suitable conditions for this type of experiment, but neutron-induced fission is not without interest, particularly as a knowledge of prompt neutron angular distributions is relevant to precision determinations of fission cross-sections made with neutron detectors.

If the prompt neutron component emitted from the moving fragment is assumed to have an isotropic angular distribution in the fragment rest system, its laboratory angular distribution can be expressed as

$$G(\theta) = G_o \left[1 + \sum_{L=1}^{\infty} G_L P_L (\cos \theta) \right]$$

where the effect of incident momentum has been neglected, so that a common fragment axis can be defined in the laboratory system, and θ is the angle between the direction of the emitted neutron and this axis. The distribution has been averaged over all prompt neutron energies.

The moments, G_L, depend on the prompt neutron energy spectrum and the division of neutron yield and total fragment kinetic energy between the light and heavy fragments. If the known fragment angular distribution is expressed as

$$W(\alpha) = W_o \left[1 + \sum_{L=1}^{\infty} W_{2L} P_{2L} (\cos \alpha) \right]$$

where α is the angle between the incident beam and the fragment axis, it can be shown that the neutron component emitted from the fragments will have an angular distribution

$$N(\phi) = 4\pi W_o G_o \left[1 + \sum_{L=1}^{\infty} \left\{ W_{2L} G_{2L}/(4L+1) \right\} P_{2L} (\cos \phi) \right]$$

ϕ being the angle between the emitted neutron and the incident beam. Calculations show that the neutron anisotropy, N(0)/N(90), is approximately proportional to the fragment anisotropy, W(0)/W(90), and its value is very insensitive to changes in the parameters entering into the calculation of the moments, G_L. As a typical example, the fission of ^{235}U by 2 MeV neutrons gives a fragment anisotropy of ~1.2 which would lead to a prompt neutron anisotropy of ~1.045.

Measurements of fission neutron angular distributions for neutron induced fission of ^{235}U and ^{238}U have been made on the 100 m flight path of the 45 MeV linac. A 7.9 cm diameter disc of the fissile material was surrounded by four NE213 neutron detectors, each 12 cm in diameter and placed 46 cm from the sample centre. Incident neutron energies were selected by time-of-flight up to a maximum of 2.3 MeV, and the detection of scattered neutrons was prevented by setting the neutron discriminator bias of each detector above this value. The bias increases the correlation between the directions of the fragments and the detected neutrons, and allowance is made for this effect in analysing the data. Gamma-rays from neutron capture or inelastic scattering were rejected with a pulse shape discrimination system. The detectors were inter-calibrated with the spontaneous fission neutrons from a disc shaped source of ^{252}Cf 7.9 cm in diameter placed at the sample position.

Preliminary results of the measurements on ^{238}U are shown in Figure 7. The data have been summed over 200 keV intervals of incident neutron energy ranging from 1.3 to 2.3 MeV. The curves are the result of a least squares fit to the data in which the expression for $N(\phi)$ is restricted to the $P_2(\cos\phi)$ term. Published data show the fragment anisotropy, W(0)/W(90) to fall from a value of ~1.6 around 1.5 MeV incident neutron energy to ~1.25 at 2.3 MeV. The observed neutron distributions show a similar trend. Although the results so far are too inaccurate to give a meaningful value for the isotropic component, they nevertheless indicate that any such component of energy greater than 2.3 MeV must be small.

B. Neutron resonance capture gamma-ray studies (B.W. Thomas and T.J. Haste (Oxford University))

1. $^{93}Nb(n,\gamma)^{94}Nb$ reaction [Relevant to Request Numbers: 621049, 682020, 702015, 742132]

(a) Low energy capture gamma-ray spectra

A preliminary analysis of the low energy capture gamma-ray spectra of ^{93}Nb has previously been given(1), in which the spins of several s-wave resonances were deduced, using the low-lying level population method(2,3). The analysis has been extended to cover the stronger p-wave resonances up to 1 keV energy, and the results are shown in Table 3, with those of previous measurements.

(1) UKNDC(73)P53, EANDC(UK)151L, INDC(UK)-20L.

(2) W.P. Poenitz, Z. Physik 197 (1966) 262.

(3) K.J. Wetzel and G.E. Thomas, Phys. Rev. C1 (1970) 1501.

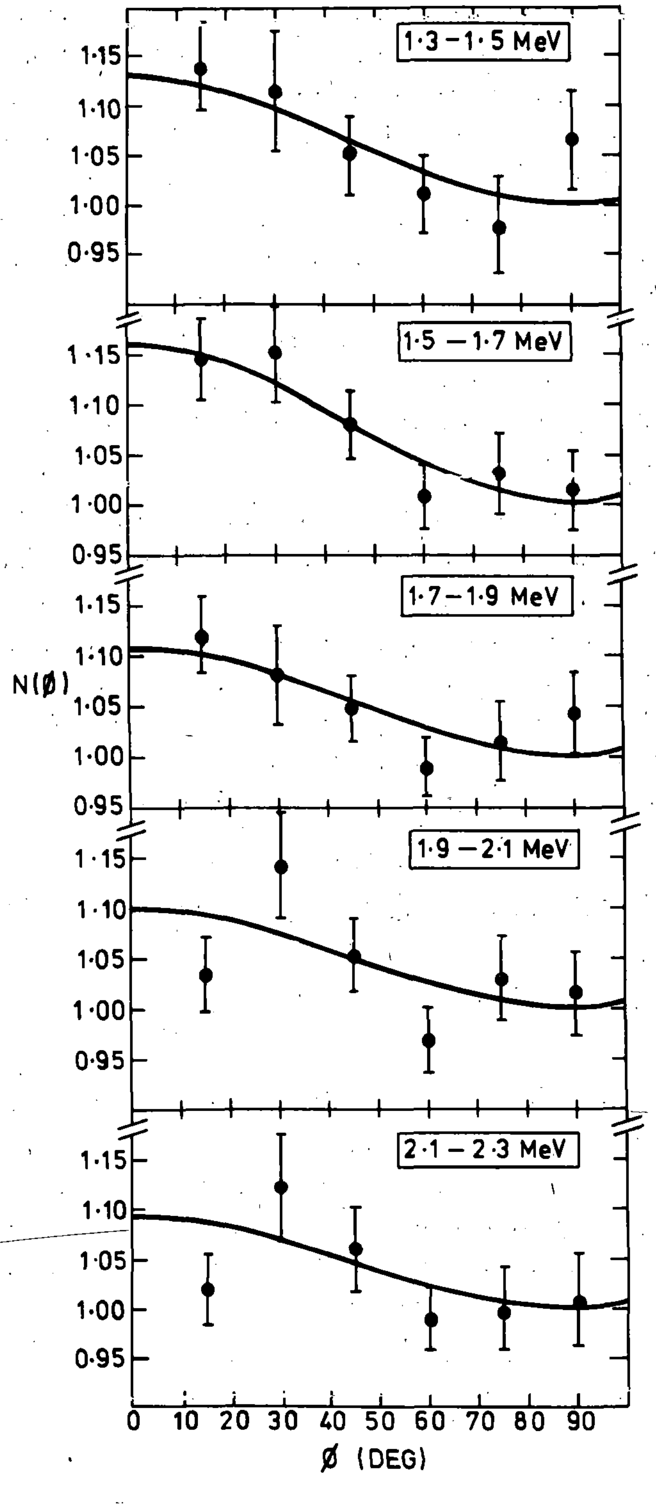

Fig. 7 Prompt neutron angular distributions from U-238 (n,f) for different intervals of incident neutron energy

TABLE 3

^{93}Nb p-wave resonance spin assignments

E_R (eV)	J				
	Prestwich et al[4] (1968)	Chrien et al[5] (1971)	Present Experiment (Low energy gamma-rays)	Present Experiment (High energy gamma-rays)	Present Experiment (Final assignment)
35.8	5	5	5	5	5
42.3	(4,5)	4	4	4	4
94.3	(3,4)	(4)	3	(3)	3
243.7		(5)	4	4	4
319.0		5	5	5	5
500.6			5	5	5
672.0			(5)		(5)
678.2			(6)		(6)
721.3				4	4
952.7				(4,5)	(4,5)
1016.4				6	6

Parentheses denote an uncertain assignment

The ratios of the 293 keV and 100 keV transitions to that at 114 keV are shown in Fig. 8, plotted against neutron energy. A dependence of these ratios on the ℓ-value as well as on the spin of the resonance is shown. No definite example of a 6^- resonance is observed below 1 keV but the spins may be determined unambiguously using the results of the high-energy capture gamma-ray experiment described below. There are no inconsistencies in the assignments.

(b) High energy capture gamma-ray spectra

Measurements have been made of the high-energy resonance capture gamma-ray spectra from the ^{93}Nb(n,γ)^{94}Nb reaction, for individual resonances up to 1 keV neutron energy, and for average regions up to 3.8 keV energy. The prime object was to investigate non-statistical effects associated with the primary transitions. A 10 cm^3 Ge(Li) detector was used at a 10 m flight path of the Neutron Booster target, and data were collected using the two-parameter system on-line to a PDP-4 computer. The target was a metal niobium disc 7.5 cm diameter of thickness 0.3 cm. Analysis of the raw data gave gamma-ray

(4) W.V. Prestwich, R.E. Coté and H. Shwe, Phys. Rev. 184 (1968) 1205.

(5) R.E. Chrien, K. Rimawi and J.B. Garg, Phys. Rev. C3, 5 (1971) 2054.

spectra for the s-wave resonances at 105.8, 119.2, 193.8, 335.5, 378.4, 460.3, 640.8 and 741.4 eV, for the p-wave resonances at 35.8, 42.3, 94.3, 243.7, 319.0, 500.6 and 721.3 eV, and for the unresolved doublets (672 + 678 eV), (935 + 953 eV) and (1009 + 1016 eV). Average capture spectra were obtained for the regions (30-1000 eV), (1000-2000 eV), (2000-3000 eV) and (3000-3800 eV). The resonances were normalised to the summed spectrum in the energy range (2.3 - 3.5 MeV) and relative gamma-ray intensities found in the range (3.9 - 7.25 MeV).

(i) Resonance spin assignments

Spin assignments deduced from primary capture gamma-rays for p-wave resonances are shown in Table 3. In addition the spins of the s-wave resonances at 105.8, 335.5 and 1009.0 eV, assigned as 4^+ in the low energy gamma-ray experiment[1] were confirmed.

(ii) Neutron binding energy and final state assignments

The neutron binding energy was determined to be 7229.0±1.5 keV from the observation of the ground state transition in several resonances. This is in good agreement with the values of Chrien et al[5] (7229.3±0.4 keV) and Jurney et al[6] (7229.5±1.5 keV). The spins, parities and energies (binding energy - E_γ) of ^{94}Nb levels up to about 1500 keV populated by primary transitions were determined. The results were combined with the assignments of Jurney et al[6] (from (d,p) studies) and the resulting level scheme is shown in Fig. 9.

(iii) Distribution of partial radiation widths

The distribution of reduced partial widths for E1 and M1 transitions in s-wave and p-wave resonances was examined using a maximum likelihood technique. The data were in all cases found to be consistent with a Porter-Thomas distribution. The sample sizes ranged from 34 to 154 reduced widths.

(iv) Correlation analysis

The reaction mechanism involved in neutron capture may be studied by investigating correlations between partial radiative widths and reduced neutron widths of the initial states, and of reduced widths of the final states, the latter being obtained as spectroscopic factors from (d,p) experiments. A correlation between transitions to pairs of final states indicates a departure from a purely statistical description of the decay process.

The data were examined for possible correlations between reduced neutron widths and partial radiation widths separately for s- and p-wave resonances of spin 4 and 5. The correlation was in all cases consistent with zero for the sample size used. In addition no significant correlation was found among radiative width pairs. This suggests that channel capture does not play a significant part in the capture mechanism. The data were also tested for correlations between the resonance averaged partial radiative widths and the (d,p) widths[6] to the same

(6) E.T. Jurney, H.T. Motz, R.K. Sheline, E.B. Shera and J. Vervier, Nucl. Phys. A111 (1968) 105.

final state. For 9 p-wave resonances and 20 final states a correlation coefficient of 0.326 was found (at the 97.3% point of the distribution when testing for zero correlation), for 9 s-wave resonances and the same final states the figures were 0.144 (81.9%). Chrien et al[5] reported values of 0.578 (99.9%) and -0.092 (32%) respectively. For average capture the coefficients were:- 1-2 keV, 0.526 (99.5%): 2-3 keV, 0.799 (>99.99%): 3-3.8 keV, 0.558 (99.8%). The high degree of correlation in the 2-3 keV neutron energy region is illustrated in Fig. 10. This positive correlation together with the absence of neutron width - partial radiative width correlations may be explained by the presence of a doorway state in this region.

2. $^{103}Rh(n,\gamma)^{104}Rh$ reaction

High energy capture gamma-ray spectra

Measurements have been made of high energy resonance capture gamma-ray spectra in the $^{103}Rh(n,\gamma)^{104}Rh$ reaction for individual resonances below 1 keV neutron energy, using the same equipment as in the niobium experiment. A sample of 100 gm rhodium metal powder in a 5 cm diameter sample holder was used as the target. The aim of the experiment was to investigate non-statistical properties associated with the primary transitions in this reaction. Analyses of the raw data are in progress.

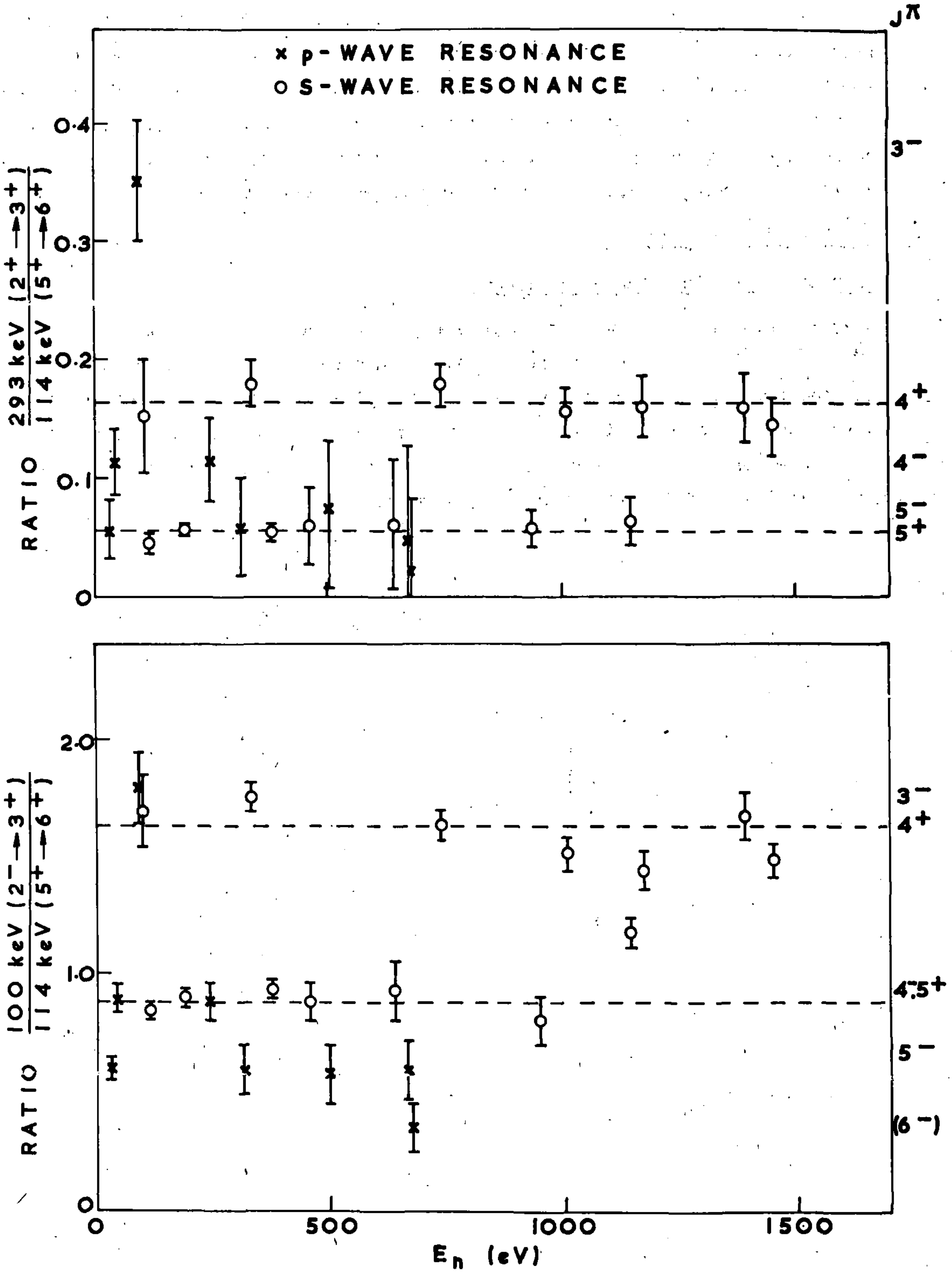

Fig. 8 Ratios of low energy γ-ray intensities in the Nb-93(n,γ)Nb-94 reaction

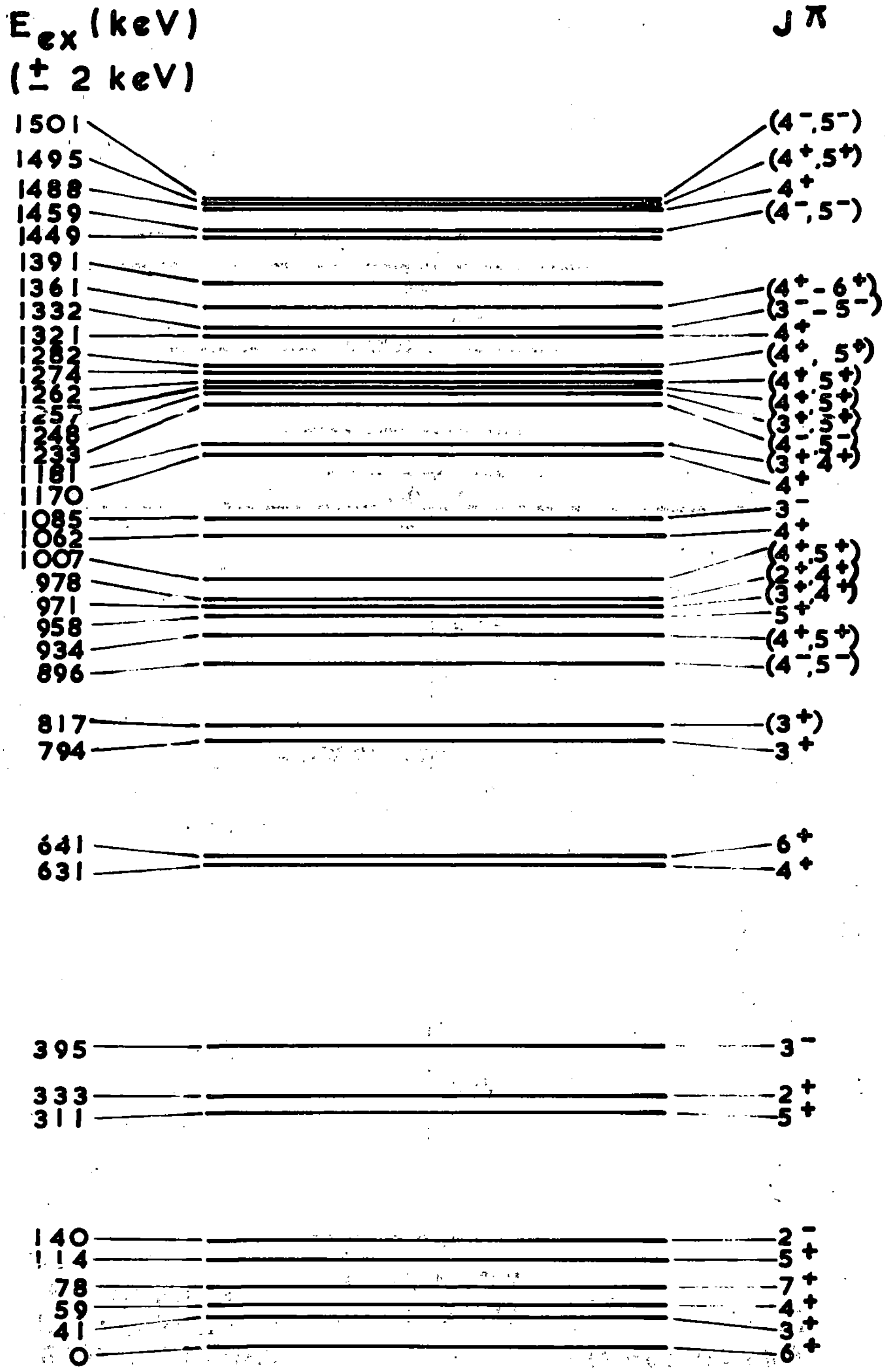

Fig. 9 Level scheme of Nb-94 (below 1510 keV)

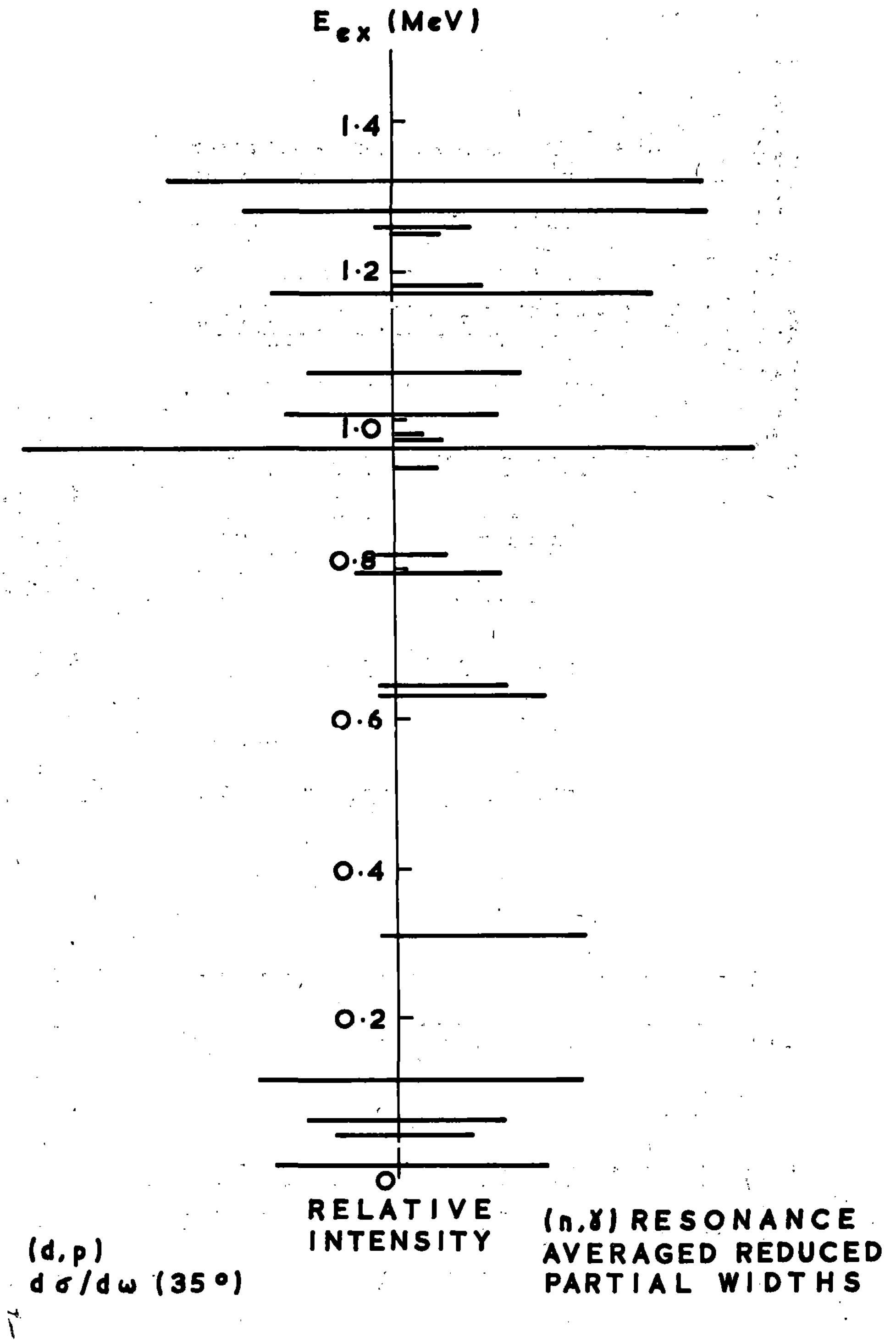

Fig. 10 Comparison of (d,p) cross-sections and (n,γ) resonance averaged reduced partial widths to the same final states in Nb-94

C. The $^{238}U/^{235}U$ fission cross-section ratio (M.S. Coates, D.B. Gayther and N.J. Pattenden) [Relevant to Request Numbers: 671203, 691416, 693064, 693065, 712067, 712068, 714020, 732112, 742036, 742112, 742136]

The analysis of the time-of-flight measurements reported previously in preliminary form[1] has now been completed. The data extend up to an energy of 22 MeV and cover a range where the conventional black resonance technique for determining time-dependent background cannot be used. However, it proved possible to assess the importance of this background component on the observed ratio by using the fission chamber to measure the transmission of carbon samples placed in the incident neutron beam. The method relies on the resonance structure in the carbon total cross-section above ~2 MeV. The background is assessed by comparing the resonance transmission shapes observed in the ^{238}U and ^{235}U sides of the chamber, and does not depend on a knowledge of the absolute carbon total cross-section. The results of the analysis are consistent with a negligible time dependent background effect and as a consequence our preliminary results above ~1.4 MeV remain unaltered. The possibility of a ±2½% systematic error due to such a background cannot, however, be precluded, and this represents the major experimental uncertainty.

The analysis of the $^{238}U/^{235}U$ fission cross-section ratio measurements has been extended to lower energies, and Figure 11 shows the data down to ~600 keV in comparison with other published results. The early values of Lamphere[2] have been re-normalised to agree with more recent measurements at higher energies, following the suggestion of Sowerby et al[3]. It can be seen that our data agree well in the threshold region with the recent values of Stein et al[4] and Meadows[5], but disagree with the Lamphere values between 600 keV and 1.8 MeV. It is interesting to note the effect this discrepancy would have on the calculated counting rate of a ^{238}U-fission chamber placed in a typical fast reactor spectrum. Taking a recently evaluated ^{235}U fission cross-section[3] to derive ^{238}U fission cross-sections from the two observed ratios, and integrating between 600 keV and 1.8 MeV in the spectrum, it is found that the rates would not differ by more than about 0.5%.

Below 600 keV, the measured cross-section ratio becomes increasingly inaccurate due to ^{235}U content of the ^{238}U fission foil (358 ppm), and meaningful results cannot be derived below 400 keV. In the energy interval 400 to 420 keV the ratio is 0.0002±0.0001 corresponding to a ^{238}U fission cross-section of 240±120 μb.

---

(1) M.S. Coates, D.B. Gayther, N.J. Pattenden, D.A. Boyce, I.T. Belcher, P.H. Bowen, J.B. Brisland, G.C. Cox and P.E. Dolley, Nuclear Physics Division Progress Report AERE - PR/NP 20, p.4 (1974), also UKNDC(73)P53, EANDC(UK)151L, INDC(UK)-20L.

(2) R.W. Lamphere, Phys. Rev. 104 (1956) 1654.

(3) M.G. Sowerby, B.H. Patrick and D.S. Mather, AERE - R 7273 (1973).

(4) W.E. Stein, R.K. Smith and H.L. Smith, Proc. Washington Conf. Neutron Cross-sections and Technology, p.627 (1968).

(5) J.W. Meadows, Nucl. Sci. and Eng. 49 (1972) 310.

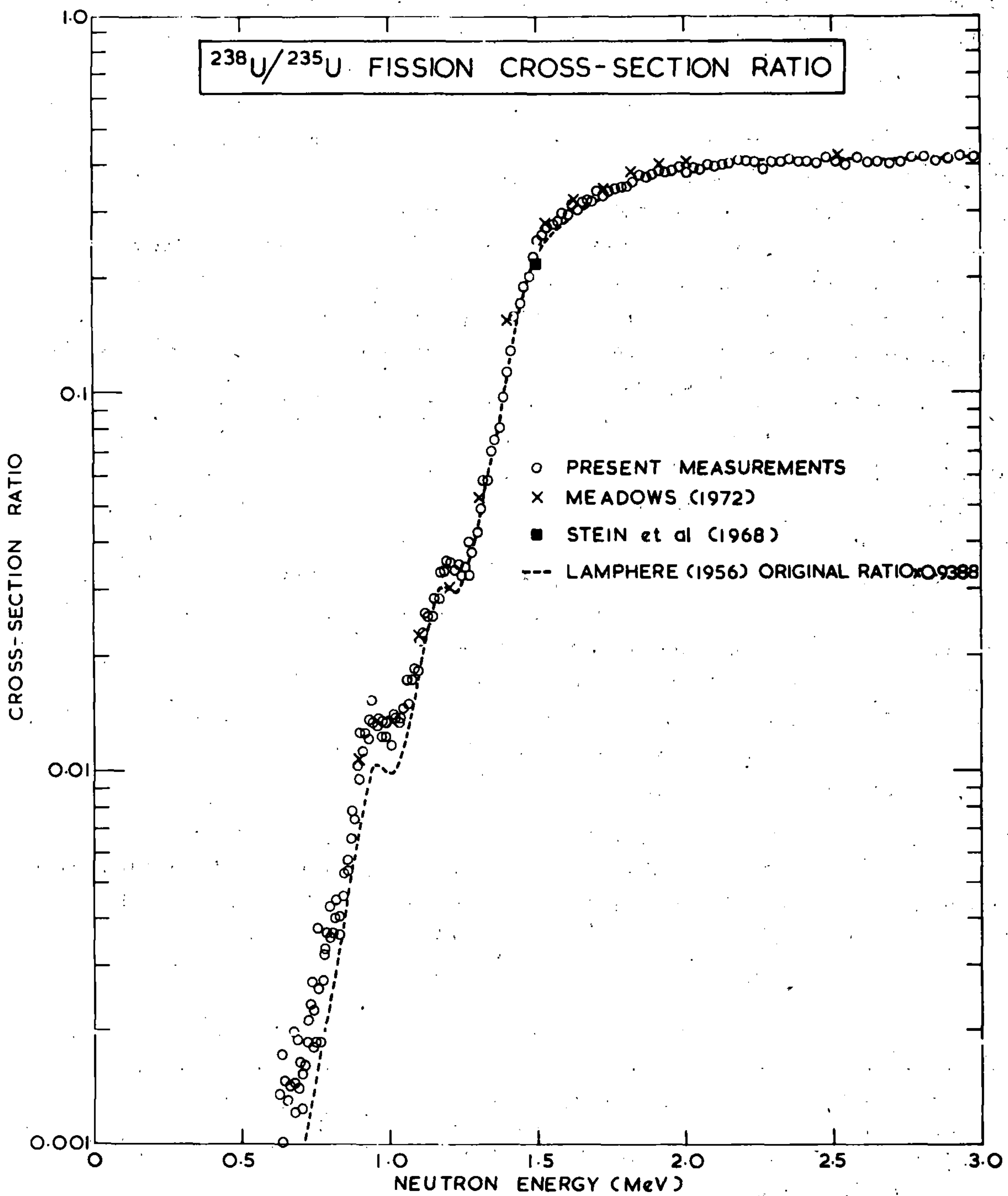

Fig. 11 U-238/U-235 fission cross-section ratio

C. High resolution neutron total cross-section measurements on the synchrocyclotron

(P.H. Bowen, P.E. Dolley, G.D. James, J. Scrivens, B. Syme, B. Thom, I.L. Watkins)
[Relevant to Request Numbers: 712021, 714003, 721038, 721047]*

Measurements of total cross-section by neutron time-of-flight experiment were resumed in December after the installation of the redesigned Dees. It was shown that these have resulted in a major reduction in the radial oscillation of the beam and thereby eliminated the afterpulses that had previously occurred. Additional collimation has improved the ratio of signal to background and enabled measurements to extend down to 1 keV. Below 5 keV, however, there are dips in the open beam caused by resonances in the tantalum face of the moderator tank. Replacement of the tantalum by beryllium is being considered.

Measurements of the total cross-section of natural iron (sample thicknesses of 1.2 cm and 3 cm) and of natural nickel (sample thickness of 0.6 cm and 1.8 cm) have been made and the background versus energy curve has been carefully determined using many resonances in the range 28 keV to 440 keV. Resonance analysis of these data is in progress.

The several areas of improvement are described in more detail below.

1. Deflection and target system

As a result of the redesign of the Dees, the deflector plates had to be raised. The proton beam profile after deflection is now roughly elliptical, of maximum extent 7 cm in the radial direction and 2 cm in the vertical direction. Nearly all the deflected beam hits the target on the first orbit after deflection. For gamma flash pulse widths in the range 5 ns to 15 ns, the optimised neutron output is a linear function of pulse width. Since the Dee modifications no pulses narrower than 5 ns have been obtained. The neutron production target and moderator have been re-designed to improve the neutron intensity.

2. Collimation and shielding

A brass collimator has been installed three metres from the proton target and the main collimator at 50 m has been lined with brass and faced with boron loaded wax. As a result, the signal to background ratio has been improved and is typically 14 to 1 for the open beam at 28 keV.

3. Electronics

The time digitizer is working satisfactorily at average rates of about one count per burst.

4. Neutron detector

The dead time associated with the ^{6}Li glass neutron detector has been reduced to 350 ns and stabilized. Other improvements and the use of other detectors are under investigation.

---

*This work is necessary to satisfy the following request numbers for capture cross-section measurements: 691103, 692101, 692102, 692103, 692104, 712024, 714005, 721039, 721043, 742032, 692128, 692129, 692131, 702009.

5. Data handling

Additions to the data processing program DPP32 have been made which enable it to work in the presence of changes in timing channel widths. A version of the Harvey-Atta program, obtained from Geel, has been made to work on the Harwell computer and is being used for resonance analysis.

Intermediate Structure in the Neutron-Induced ^{235}U Cross-sections

(G.D. James, G. de Saussure (ORNL), R.B. Perez (ORNL))⁄

The ^{235}U fission cross-section exhibits large fluctuations in the unresolved resonance region.(1-4) One asks whether this phenomenon can be explained in terms of the statistical nuclear model, or whether, on the contrary, these fluctuations represent departures from it, in localized energy regions,(5) where enhancements of the reaction widths occur.

Two statistical tests have been proposed(6,7) to determine whether these fluctuations are of a random nature: the Wald-Wolfowitz(8) and the Levene-Wolfowitz(8) tests. In the former, one counts the number of runs, R, of consecutive observed values which lie above or below a reference value (ideally the median); in the latter, one counts the number of consecutive observed pairs of values of increasing or decreasing magnitude (runs up or down), thus creating a set of runs, $R(\ell)$, of length, ℓ. Both statistics provide the number of runs, E(R), expected from random statistical data, as well as the standard deviation, $\sigma(R)$, and the probability, P(R), for R to depart from its expected value by more than F standard deviations.

To utilize these tests with confidence, one has to prove that cross-sections obtained from the statistical nuclear model do indeed satisfy both statistics. The ^{235}U fission cross-section was simulated by Monte Carlo techniques for neutron energies between 10 and 40 keV, and averaged over 100-eV energy intervals. The results of the statistical tests given in the top row of Table 4 show the adequacy of both statistics.

The capability of detecting the presence of intermediate structure was tested by mocking up fission width enhancement on the basis of the double-humped fission barrier

---

⁄ Work done while G.D. James was visiting the Oak Ridge National Laboratory.

(1) B.H. Patrick et al., J. Nucl. Energy, 24, (1970) 269.

(2) J.R. Lemley et al., Nucl. Sci. Eng., 43, (1971) 281.

(3) C.D. Bowman et al., Proc. Second Conf. Nuclear Data for Reactors, Helsinki, IAEA (1970).

(4) G. de Saussure et al., Trans. Am. Nucl. Soc., 14, (1971) 370.

(5) C. Mahaux, Statistical Properties of Nuclei, p. 545, J.B. Garg, Ed., Plenum Press, New York (1972).

(6) G.D. James, Nucl. Phys., A170, (1971) 309.

(7) Y. Baudinet-Robinet and C. Mahaux, Phys. Letters, 42B, (1972) 392.

(8) A. Wald and A. Wolfowitz, Annal Math. Stat., X1, 2 (1940); also Documenta Geigy, Scientific Tables, Geigy Pharmaceuticals, Ardsley, New York, K. Kiem, Ed.

model.[9] In this case the fission widths, $\Gamma_{\lambda'f}$, of fine structure resonances (Class I levels) are modulated by the presence of levels in the second fission potential barrier minimum[10] (Class II levels) according to the equation[11]

$$\Gamma_{\lambda'f} = \Gamma_{\lambda f} + \sum_{\mu} \frac{A_{\lambda\mu}^2 \Gamma_\mu}{(E - E_\mu)^2 + (1/4)\Gamma_\mu^2} \qquad (1)$$

where $\Gamma_{\lambda f}$ belongs to the Class I levels, Γ_μ and E are the fission widths and level energies for the Class II levels, and $A_{\lambda\mu}$ is the coupling between the two potential wells. It can be seen from rows 2 and 3 of Table 4 that the data generated according to Eq. (1) show large departures from random statistical behaviour in both statistical tests.

Next, the ^{235}U-fission and capture cross-sections measured at ORELA were averaged over 100-eV intervals between 10 and 40 keV and tested as shown in Table 4. The significant deviations from random statistical behaviour confirms the presence of an intermediate structure in both the ^{235}U fission and capture cross-sections. This finding has implications in regard to our understanding of the unresolved resonance region and treatment of cross-sections in this region for reactor design.

(9) V.M. Strutinsky, Nucl. Phys. A95, (1967) 420.

(10) J.E. Lynn, AERE - R 5891, Atomic Energy Research Establishment (Sept. 1968).

(11) R.B. Perez et al., "Simultaneous Measurements of the Neutron Fission and Capture Cross Sections for ^{235}U for Neutron Energies from 8 eV to 10 keV", ORNL-TM-3696, Oak Ridge National Laboratory (1972).

Intermediate Structure Studies of ^{234}U Cross-sections (G.D. James, J.W.T. Dabbs (ORNL), J.A. Harvey (ORNL), N.W. Hill (ORNL) and R. Schindler (ORNL))⸸

1. Introduction

The high resolution measurements of the neutron induced fission and total cross-sections of ^{234}U, carried out by time-of-flight measurement on ORELA, have been analysed with the aim of (i) determining the neutron widths Γ_n and fission widths Γ_f for all observed fine structure resonances below 1.5 keV which form the major part of a narrow intermediate structure resonance centred at about 638 eV[1,2], (ii) to improve our knowledge of other low energy class II levels and of the class II level spacing D_{II} and (iii) to study the cross-section fluctuations[3], near a supposed vibrational level at 310 keV, with improved statistical accuracy. From an analysis of the data near 310 keV, on the assumption that a vibrational level at this energy gives fission strength to class II levels at lower energy, it is deduced that the average class II fission width at low energy is 0.0074 eV whereas the measured values differ from this by three standard deviations. This result indicates that the low energy levels also derive strength by the direct coupling of the Class I and Class II levels.

⸸ Work done while G.D. James was visiting Oak Ridge National Laboratory.

(1) G.D. James and E.R. Rae, Nucl. Phys. A118, (1968) 313.

(2) G.D. James and G.G. Slaughter, Nucl. Phys. A139, (1969) 471.

(3) G.D. James, A. Langsford and A. Khatoon, Progress Report AERE - PR/NP 19, p16.

TABLE 4

Results of Tests for Intermediate Structure in U-235 Cross-Sections

Cross-section tested	Type of data	Wald and Wolfowitz Statistics					Levene and Wolfowitz Statistics				
		R	E(R)	σ(R)	F	Probability P(R)	R(1)[a]	E(R1)	σ(R1)	F	Probability P(R)
σ_{nf}	Simulated (no modulation)	149	151.0	8.65	0.17	0.43	122	123.0	11.2	0.043	0.48
σ_{nf}	Simulated (with modulation)	79	143.3	8.20	7.78	$<10^{-7}$	90	120.9	11.1	2.74	3.04×10^{-3}
$\sigma_{n\gamma}$	Simulated (with modulation)	67	150.0	8.59	9.61	$<10^{-7}$	92	123.8	11.2	2.79	2.62×10^{-3}
σ_{nf}	Measured	94	150.2	8.60	6.48	$<10^{-7}$	85	123.4	11.2	3.38	3.6×10^{-4}
$\sigma_{n\gamma}$	Measured	122	150.7	8.62	3.27	5.4×10^{-4}	110	123.8	11.2	1.19	0.117
$\sigma_{n\gamma}/\sigma_{nf}$	Measured	126	150.9	8.64	2.82	2.37×10^{-3}	111	123.8	11.2	1.10	0.136
$\sigma_{n\gamma} + \sigma_{nf}$	Measured	109	150.8	8.63	4.79	85×10^{-7}	111	123.4	11.2	1.06	0.144

(a) Only the runs of length, $\ell = 1$, are shown.

2. Fine structure level parameters

The neutron and fission widths of 118 levels observed below 1.5 keV have been derived from a Harvey-Atta area analysis of the total cross-section and using the measured areas of each fission cross-section resonance. After correcting for missed levels on the assumption of a Porter-Thomas distribution of reduced neutron widths, the class I level spacing $D_I = 10.64 \pm 0.46$ eV and the s-wave strength function $\langle\Gamma_n^{\,o}\rangle/D_I = (0.857 \pm 0.108) \cdot 10^{-4}$. In Fig. 12 we show the energy dependence of the fission widths below 1.5 keV. It can be seen that there are large values of the fission width at 1092.5 and 1134 eV and it is possible that these could arise because of a second narrow intermediate structure level at about this energy. The data have therefore been analysed under the assumption that the fission widths are distributed with a χ^2 distribution with ν degrees of freedom about a mean value ($\langle\Gamma_f\rangle$) given by the expression

$$\langle\Gamma_f\rangle = \frac{K}{(E - E_{II})^2 + \frac{W^2}{2}} + \frac{K_2}{(E - E_{II2})^2 + \frac{W_2^{\,2}}{2}}$$

A method of estimating the parameters has been evolved which minimizes the quadrature sum of the number of standard deviations by which each of three statistics are away from their expectation values. These statistics are (i) the statistic, $F(^{\nu}/2)$, associated with the fit to a χ^2 distribution(4), (ii) the Wald and Wolfowitz runs statistic, U,(5) and (iii) the number of points above the median. The results of the fit are given in Table 5 which shows that the combined error is a minimum for two class II levels. However, the presence of a second level cannot be confidently inferred from this result without carrying out an analysis of variance.

3. Class II levels below 15 keV

There is clear evidence for narrow intermediate structure levels at 550, 1092, 3100, 4575, 7845, 11886 and 13072 eV giving a class II level spacing $D_{II} = 2.1 \pm 0.4$ keV. For each of these levels we can derive a class II fission width, assumed equal to a sum over class I fission widths, from the average reduced neutron width. The values are, respectively, 0.0478, 0.0107, 0.0284, 0.0979, 0.4954, 0.1159 and 0.2681 eV.

4. Cross-section fluctuations near 310 keV

There is decisive evidence for strong fluctuations of the ^{234}U fission cross-section over the entire energy range shown in Fig. 13 as well as for vibrational levels at 310 keV, 550 keV and 750 keV. Average parameters for the fluctuation structure near 310 keV are given in Table 6, together with average parameters of cross-sections simulated by Monte Carlo methods. These simulated results are for double humped barrier parameters $V_A = 63.5$ keV and $V_B = 590$ keV and are in good agreement with the measured values. (V_A and V_B are the heights of the intermediate and outer fission barriers above the neutron binding energy). However, the barrier parameters quoted give $\langle\Gamma_{fII}\rangle = 0.0074$ eV at 1 keV which indicates that the low energy class II levels also derive strength by coupling other than through a vibrational level at 310 keV.

---

(4) C.E. Porter and R.G. Thomas, Phys. Rev. 104, (1956) 483.

(5) A. Wald and A. Wolfowitz, Annals Math. Stat. XI, No. 2 (1940); see also G.D. James, Nucl. Phys. A170, (1971) 309.

TABLE 5

Lorentzian Fit to ^{234}U Fission Width Data

Number of Class II Levels	E_{II} E_{II2} (eV)	W W_2 (eV)	K K_2 (meV.eV^2)	$F(\nu/2)$	Associated value of ν	Wald-Wolfowitz Error≠	Number of Points Above Median	Associated Binomial Error≠	Total Combined Error≠
1	550	220	34895	-1.173	1.07 ± 0.14	1.176	56	0.552	1.395
1	650	200	32849	-1.175	1.07 ± 0.14	1.569	60		1.646
2*	550 1092.5	125 ± 43 105 ± 33	11919 5856 ± 3354	-1.268	1.0 ± 0.14	0.832	59	0.0	0.832
2	600 1092.5	105 103	9122.9 7037.6	-1.177	1.07 ± 0.14	1.663	65	1.10	1.21
2	550 1050	125 400	14333 16903	-1.372	0.93 ± 0.13	0.643	51	1.47	1.66

≠ Number of standard deviations

* Preferred fit

TABLE 6

Comparison of Experimental and Simulated Structure

	Experimental Data	Simulated Results+
Vibrational level width	50 keV	59 ± 4 keV
Average peak cross-section	0.0725 b	0.0854 ± 0.0117 b
Average structure height	0.088 ± 0.011 b	0.081 ± 0.0053 b
Average structure width	4.6 ± 0.5 keV	3.68 ± 0.23 keV
Average structure spacing	10.0 ± 2.1 keV	9.7 ± 0.7 keV

+ For V_B = 590 keV.

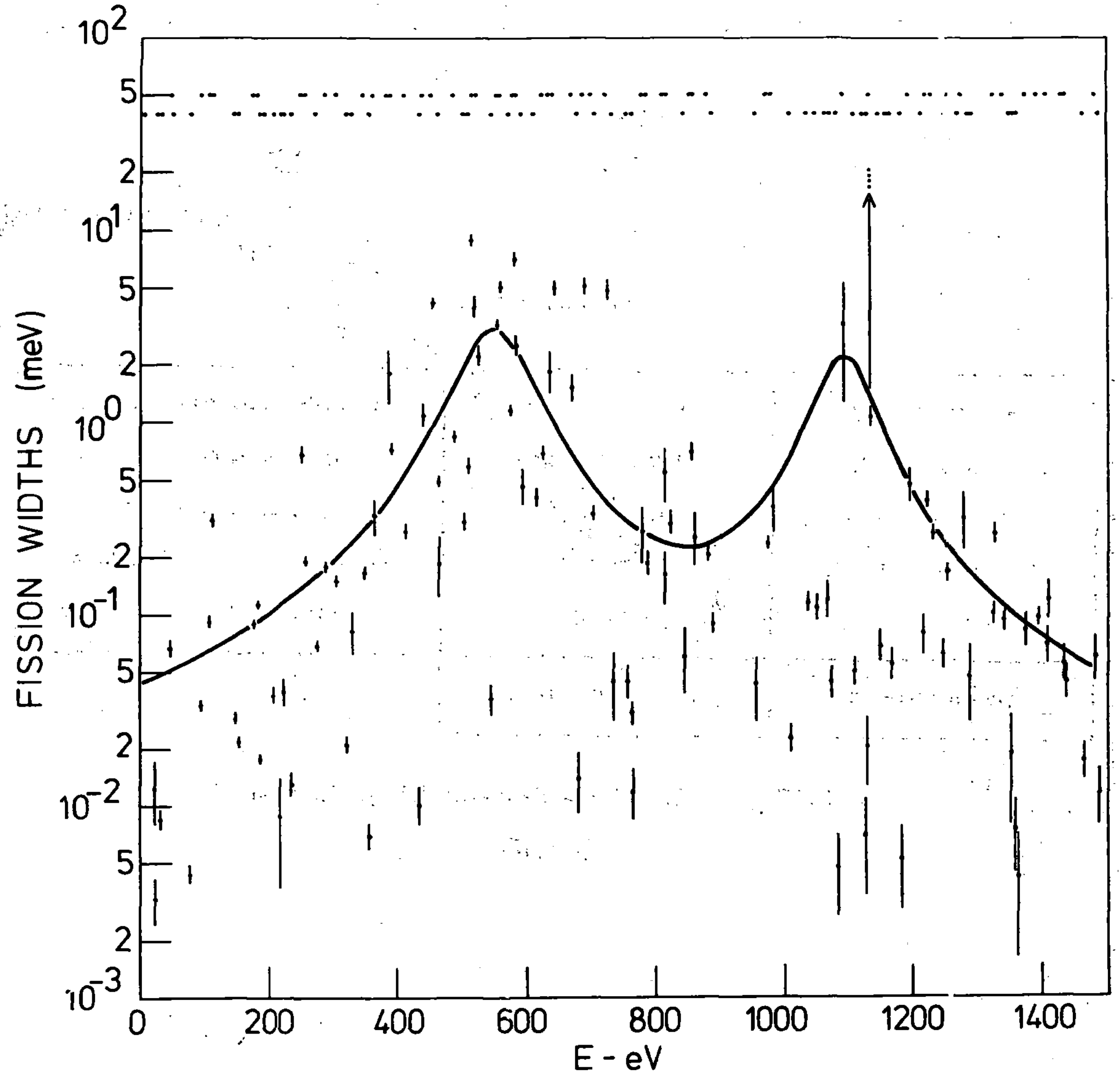

Fig. 12 The fission widths of ^{234}U + n resonances as a function of incident neutron energy below 1.5 keV. The curve is the preferred fit referred to in the text

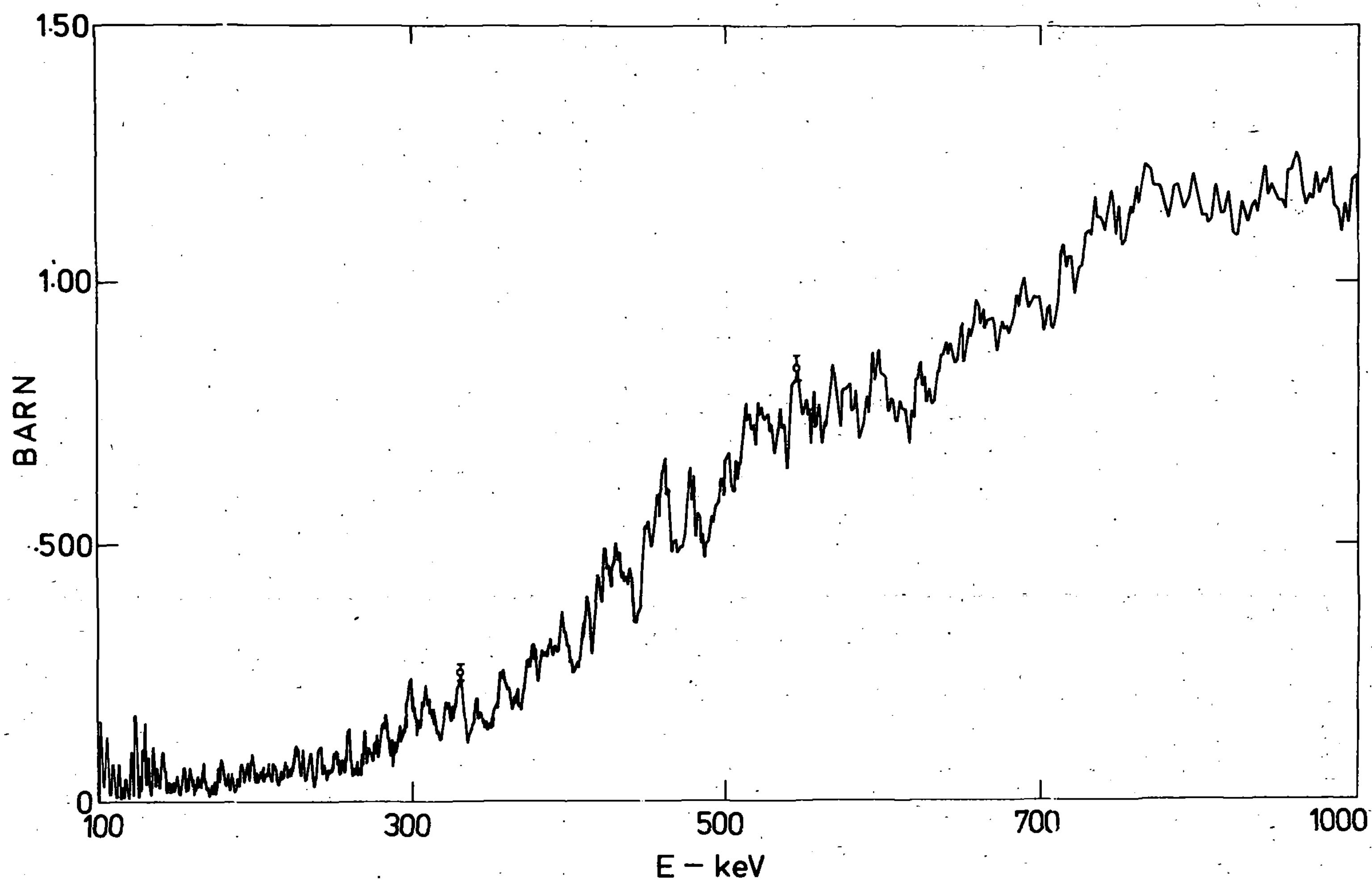

Fig. 13 The measured ^{234}U fission cross-section as a function of incident neutron energy from 100 keV to 1 MeV

Revision of the simultaneous evaluation of the fission cross-sections of ^{235}U, ^{238}U and ^{239}Pu and the capture cross-section of ^{238}U in the energy range 100 eV to 20 MeV

(M.G. Sowerby, B.H. Patrick with D.S. Mather (AWRE))

The simultaneous evaluation of the fission cross-sections of ^{235}U, ^{238}U and ^{239}Pu and the capture cross-section of ^{238}U, which was discussed in a previous progress report(1) and fully documented in a Harwell report(2), has been revised taking into account all new measurements published in final form before 1st January 1973 and some selected data which have become available since then.

The most significant change in the recommended values is in the capture cross-section of ^{238}U above 100 keV where previously higher weight had been given to the values measured relative to the fission cross-section of ^{235}U than to the absolute capture measurements. The accurate data of Ryves et al(3) however showed that the direct determinations are not now compatible with those measured relative to the fission cross-section of ^{235}U, the latter suggesting cross-section values typically 15% higher than the former in the energy range 100-800 keV. Since we believe that the uncertainty in the ^{235}U fission cross-section cannot be responsible for this discrepancy, it was judged no longer reasonable to include both types of data in the simultaneous fit. In the revised evaluation we have therefore essentially eliminated the ratio data by giving them extremely low weight and this has caused the recommended values of the capture cross-section to be significantly lower than the earlier ones above 100 keV. Although we believe that the cross-section values given by the direct measurements are more likely to be correct than the higher values suggested by the ratio data, we cannot find any reason why the latter should be in error. In placing the blame for the discrepancy on the ratio data, we are simply making a judgement on the probable cause of the problem.

The revision has resulted in small changes, within the previously estimated errors, being made to the evaluated fission cross-sections. The inclusion of new data has enabled the estimated uncertainties on the cross-sections to be generally reduced by significant amounts.

The revised evaluation has been accepted for publication by the "Annals of Nuclear Science and Engineering".

---

(1) UKNDC(72)P37, EANDC(UK)140AL, INDC(UK)15G.

(2) M.G. Sowerby, B.H. Patrick and D.S. Mather, AERE - R 7273.

(3) T.B. Ryves, J.B. Hunt and J.C. Robertson, J. Nucl. Ener. 27 (1973) 519.

Estimates of the (n,γn') cross-section for ^{238}U (J.E. Lynn)

In fast neutron reactions the possibility exists of neutron capture followed by emission of a primary gamma-ray of sufficiently low energy that the final state in the transition of the excited nucleus still lies considerably above the neutron separation energy, in which case the most probable subsequent mode of de-excitation (in non-fissile nuclei) is neutron emission to one of the low-lying states of the residual nucleus (see Fig. 14). The possibility of this process was recognised in early theoretical calculations on the neutron capture process[1], but Moldauer[2] first drew attention to its possible role in fast reactor physics as an additional neutron moderating mechanism. In later work on the neutron spectrum of ceramic-fuelled fast reactor type integral assemblies there has nearly always been difficulty in reconciling calculation with experimental measurements of the spectrum at low neutron energies without lowering the differential ^{238}U capture cross-section data by what seems an almost unacceptable amount. For this reason interest in the (n,γn′) moderating mechanism has revived recently. In particular, Fricke and Neill[3] have produced estimates for the cross-section of the (n,γn′) reaction that seem surprisingly large, but do have the ability to explain the low energy neutron spectra (below about 10 keV) of certain American fast integral assemblies like ZPR-3/11 and STSF-7 (similar to Zebra-1) while using experimental ^{238}U capture data. In view of this reported success, it is desirable to make independent estimates of this cross-section and to assess the degree of model dependence of the calculation.

Such calculations have now been carried out using level density relations and radiation mechanisms developed for the general assessment of higher energy cross-sections for the actinide nuclei. Two possible radiation models have been employed in these calculations, one being a simple electric dipole model in which the radiative strength of a transition is simply proportional to the cube of gamma-ray energy, and the other being the dipole giant resonance model which favours the emission of rather harder primary gamma-rays. There is a considerable difference between these models in their implications for the magnitude of the (n,γn′) reaction (see Fig. 15) but nevertheless they both fall far short of the estimates given in references (2) and (3), and indeed the process would appear to fail to account for the low energy spectra measured in fast reactor integral experiments by at least two orders of magnitude.

---

(1) A.M. Lane and J.E. Lynn, Proc. Phys. Soc. A70 (1957) 557.

(2) P.A. Moldauer, Proc. Conf. on Neutron Cross-section Technology, CONF-660303, Vol. 2, p.613, USAEC (1966).

(3) M.P. Fricke and J.M. Neill, Nucl. Sci. and Tech. 10, No. 7 (1973) 392.

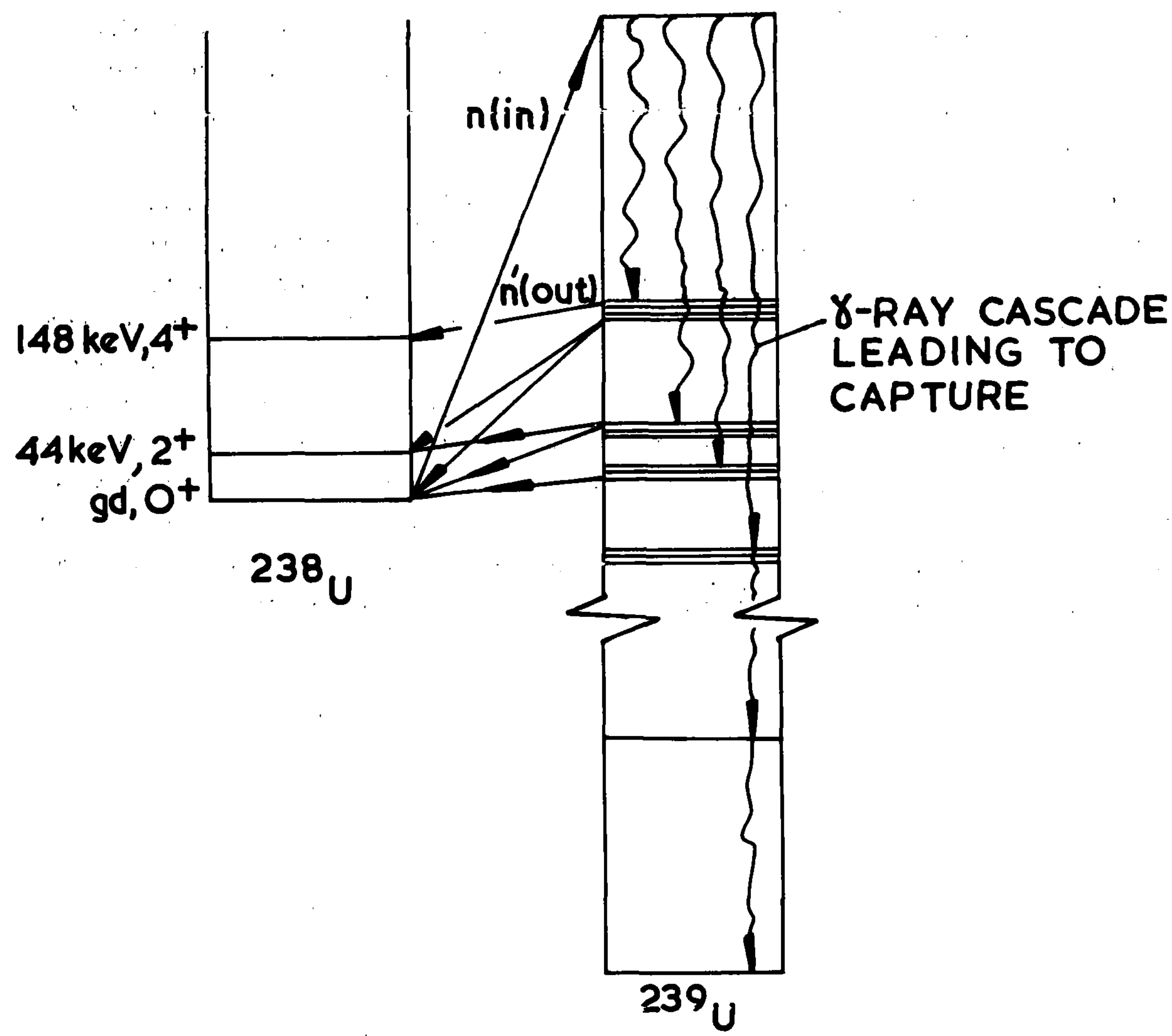

Fig. 14 Schematic diagram of cascades for (n,γn') and (n,γ) capture reactions

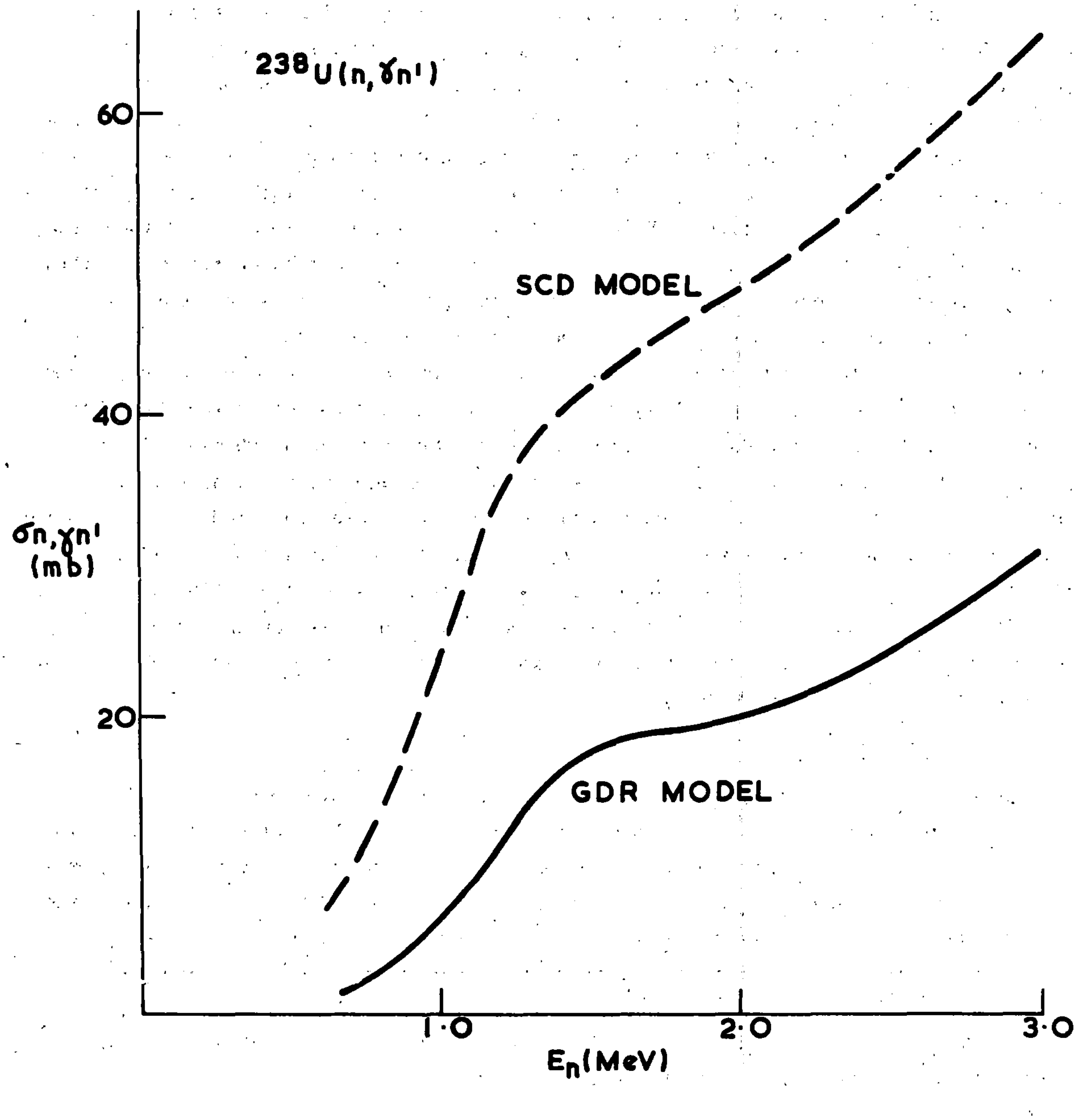

Fig. 15 Total cross-section of the (n,γn') reaction as a function of incident neutron energy

The effect of the double-humped fission barrier on energy-averaged fission probability (J.E. Lynn)

For many actinide nuclei the fission barrier (defined as the higher peak of a double-humped barrier shape) lies below the neutron emission threshold. A whole series of measurements of the fission probability (as a function of excitation energy) of such nuclei below the neutron threshold have now become available, the fissioning nucleus having been excited by (d,p), (t,p) and similar transfer reactions. In these cases only the weak electromagnetic radiation process is in competition with fission, so that strong falls in the fission probability with decreasing excitation energy are only observed some considerable energy below the barrier, and careful interpretation is therefore necessary to deduce from such data the true barrier height. A common procedure has been simply to compute the average fission width through the double barrier and equate the fission probability to the ratio of this average width to the sum of the fission and radiation widths. Below the barrier this procedure can be erroneous, for the fission width will then be concentrated locally into narrow energy bands (the class-II resonances) outside of which the radiation process competes much more effectively with fission, and this will bring the beginning of the strong fall in fission probability much closer to the barrier than would be calculated from the cruder method. Expressions for the fission probability incorporating this structure effect have been worked out in terms of the double-barrier parameters and have been published in a joint paper with B.B. Back of the Niels Bohr Institute, Copenhagen (J. Phys. A, Vol. 7 (1974) 395). This method is now being used to analyse the new fission data induced by transfer reactions mentioned above as well as in a re-analysis of sub-barrier neutron-induced fission to give a revised assessment of fission barriers. As well as being of intrinsic nuclear physics interest, these barrier assessments and their systematics are of importance in the calculation of unmeasured cross-sections of many actinide nuclei that may feature in reactor technology.

Data for Fusion Reactors (A.T.G. Ferguson)

In line with the policy previously reported(1) work has proceeded to build up the neutron physics facilities on the Tandem Generator. The first experimental work using these is the study of (n,p) scattering described below. In parallel with this, work is beginning on the evaluation of nuclear data in the range 3-14 MeV for the common structural materials. This will provide the basis for future programmes.

(1) UKNDC(73)P53, EANDC(UK)151L, INDC(UK)-20L.

D. Scattering of Fast Neutrons by Protons (J.A. Cookson, J.L. Fowler (ORNL), M. Hussain (Univ. of Dacca) and C.A. Uttley) [Relevant to Request Number: 721001]

The Harwell tandem accelerator is being used in a measurement of the angular distribution for H(n,n)H scattering between 14 and 28 MeV. This cross-section is of course a most important standard upon which many other cross-sections are based. However, recent analysis(1) of existing data and calculations based on phase shifts obtained at higher energy indicates that in the region of 5 to 30 MeV the centre-of-mass angular

(1) J.C. Hopkins and G. Breit, LA-DC-11153, also Nuclear Data Tables, A9 (1971) 137.

distributions disagree appreciably with the familiar Gammel formula: $\sigma(180^{o})/\sigma(90^{o}) = 1 + 2(E/90)^{2}$ and that there are also significant (~6% at 10 MeV, ~10% at 20 MeV) forward-backward asymmetries which have been hitherto largely ignored.

The present experiment is intended to measure the angular distribution for scattering neutrons into the forward hemisphere of the centre-mass system for at least two energies - 20 MeV and 28 MeV are currently favoured.

The experiment falls naturally into two parts of which one is the actual scattering measurement shown in Fig. 16. This consists of neutrons produced at 0^{o} by the T(d,n) reaction being scattered in a 3 cm diameter plastic scintillation detector and then detected 80 cm away by a larger scintillation detector. Since the smaller scintillator will be almost 100% efficient in detecting recoil protons corresponding to neutrons scattered towards the larger detector, the number of events with the correct flight time between the two detectors will be a measure of the scattering cross-section at that particular angle combined with a factor for the large detector's efficiency.

The second part of the experiment is illustrated in Fig. 17 and shows the associated particle method being used to measure the large detector's efficiency. Three angles for observation of associated particles have been chosen to allow the efficiency to be calibrated over a wide energy range using both the $T(d,n)^{4}He$ and $D(d,n)^{3}He$ reactions. This part of the system is expected to be a valuable facility apart from its use in the present experiment.

The current status of the measurement is that both parts have been tried out on the tandem and no insuperable difficulties have been identified. The aimed-for accuracy of 3% in the relative angular distributions still appears feasible. The immediate technical problem is in the detector calibration where the silicon barrier detectors tried so far have failed to distinguish the associated particles sufficiently well from more energetic particles of lower ionizing power. The use of thin fully depleted detectors is being considered.

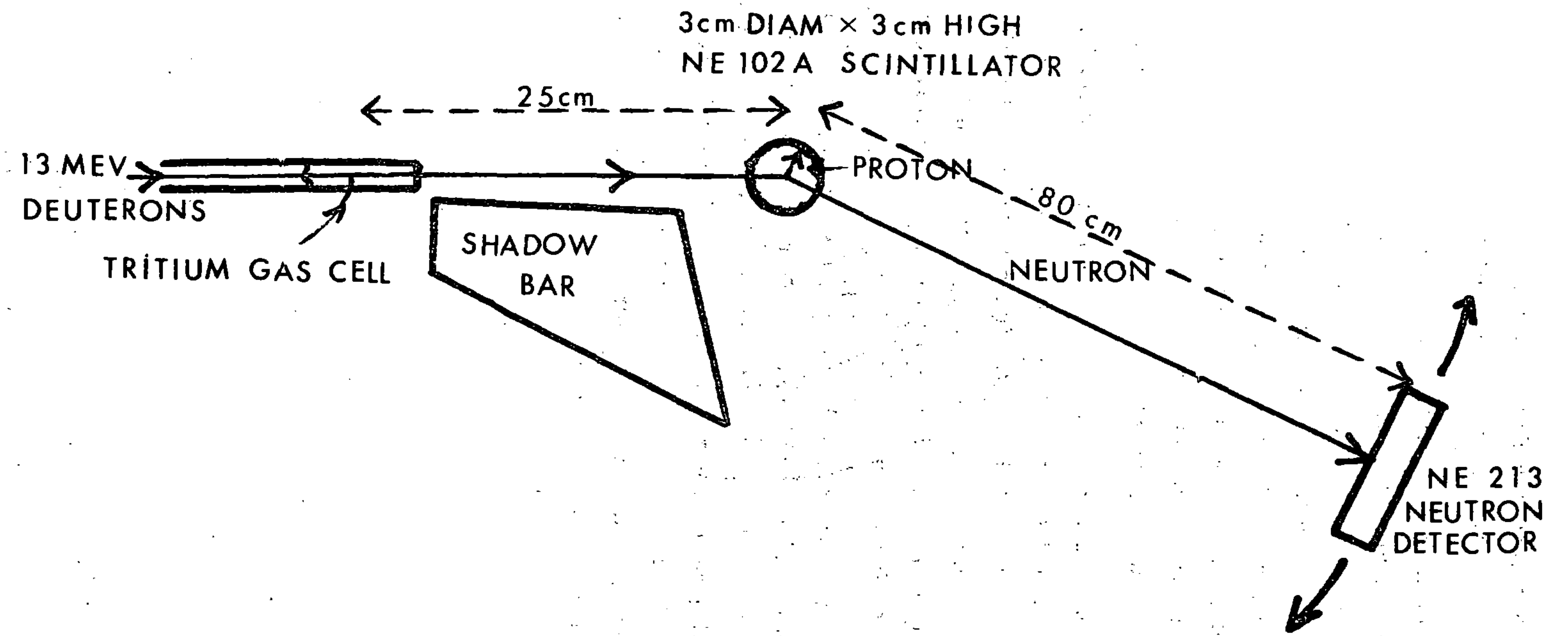

Fig. 16 Measurement of the angular distribution of neutrons scattered by protons

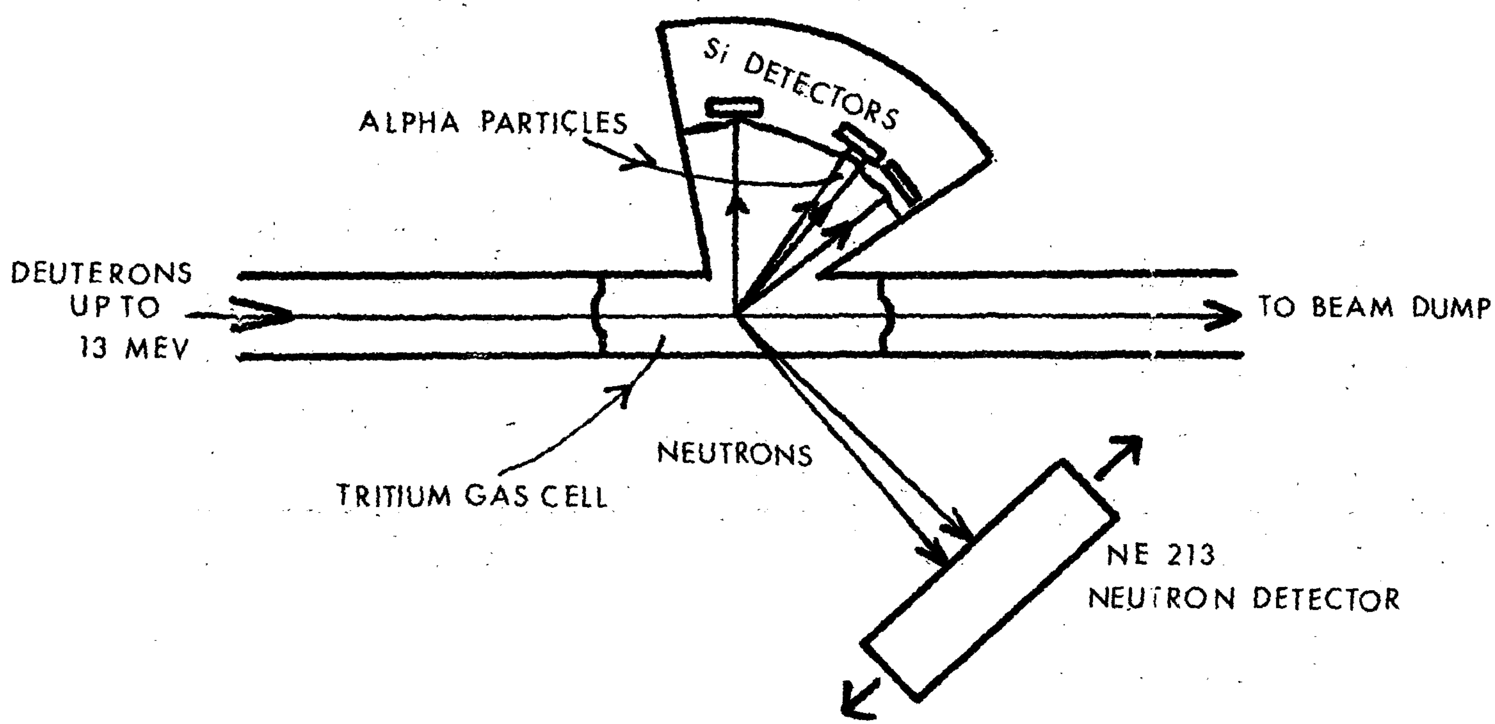

Fig. 17 Calibration of neutron detector efficiency by an associated particle method

REPORTS

AERE - R 7373 Some background and interference characteristics of intermediate structure in the fission reaction.
J.E. Lynn.

PUBLICATIONS

Sub-barrier fission probability for a double-humped barrier. J.E. Lynn and B.B. Back, J. Phys. A 7 (1974) 395.

IN COURSE OF PUBLICATION

A simultaneous evaluation of the fission cross-sections of ^{235}U, ^{239}Pu and ^{238}U and the capture cross-section of ^{238}U in the energy range 100 eV to 20 MeV.
M.G. Sowerby, B.H. Patrick and D.S. Mather.
Annals of Nuclear Science and Engineering.

CONFERENCE PAPERS

Contributed

EACRP-EANDC Specialists Meeting on Capture in Structural Materials, Karlsruhe, May 1973.

Some problem areas in capture cross-section measurements.
M.C. Moxon, D.B. Gayther and M.G. Sowerby.

Neutron cross-sections of natural nickel and its isotopes below a neutron energy of 600 keV.
M.C. Moxon.

Subthreshold fission of ^{234}U. J.W.T. Dabbs, G.D. James and N.W. Hill. Bull. Am. Phys. Soc. (Washington D.C., April 1974).

Neutron total cross-section of ^{234}U. J.A. Harvey, G.D. James, N.W. Hill and R.H. Schindler. Bull. Am. Phys. Soc. (Washington D.C., April 1974).

Neutron Fission Cross-section of ^{249}Cf. J.W.T. Dabbs, C.E. Bemis, G.D. James, N.W. Hill, M.S. Moore and A.N. Ellis. Bull. Am. Phys. Soc. (Washington D.C., April 1974).

Intermediate structure in the neutron induced ^{235}U cross-sections. G.D. James, G. deSaussure and R.B. Perez. A.N.S. Trans. 17. Nov. 73.

A.E.E. WINFRITH, REACTOR PHYSICS DIVISION

(Division Head: Dr. C.G. Campbell)

Evaluation of delayed neutron yields (R.W. Smith) [Relevant to Request Numbers: 692397, 712070, 691312, 712084, 732114]

The delayed neutron yields evaluated by Tomlinson (AERE-R 6993) for ^{238}U, ^{239}Pu and ^{242}Pu have been revised to take account of revisions to the measurements by Krick and Evans, Masters et al and Clifford. The revised percentage yields (n/100F) are:-

^{238}U	4.58 ± 0.26
^{239}Pu	0.633 ± 0.026
^{242}Pu	1.5 ± 0.5

UK Nuclear Data Library (J.S. Story, A.L. Pope)

Neutron data evaluation work in the UKAEA is being reported regularly in the series of Neutron Nuclear Data Evaluation Newsletters (NNDEN), published by the CCDN. For the period under review see NNDEN 11 to 13.

An error was discovered in the data file for H in H_2O (DFN 923) at 0.125 eV; this error has been corrected, and the CCDN have been notified. A further summary of the main library tape NDL-1 has been published; AEEW-M1208 (Pope), which includes references to the data.

A comparative study has been made of the main integral characteristics of the neutron capture data in the more than 400 data files in the UK NDL format with $30 \leq Z \leq 68$, mostly fission products; AEEW-M1234 (Pope and Story). A summary of data and MINIGAL - abstract of all fission-product and associated data files in the UKNDL is in publication (Pope).

A data file for Al (DFN 935) has been produced using evaluated resonance parameters. Work commenced on Au, ^{3}He, In, Mg, Sn, ^{149}Sm, ^{155}Gd, ^{157}Gd.

A modular computer programme - ASP - (The Adjustable Sub-routine Programme) was written to manipulate UKNDL Library tapes written in binary mode, see WNDG-114 (Pope). This programme is a very versatile tool and may well prove useful to the general user of UKNDL. ASP together with most of the editing and manipulating programmes referred to in NNDEN/10 are now available in Fortran IV.

Thermal Neutron Scattering Matrices and Allied Work (A.T.D. Butland)

Graphite

A set of thermal neutron scattering matrices for graphite at 15 temperatures in the range 293°K to 3273°K, generated before March 1973 as described in the previous progress report (EANDC(UK)151L), has now been thoroughly and satisfactorily tested and is in current use. The tests included:-

(a) those of a fundamental nature, e.g. comparisons of the predicted total thermal scattering cross-section with experimental measurements; and

(b) use of the matrices in calculations for certain zero-energy graphite moderated reactor assemblies so as to determine whether particular reactor parameters, e.g. temperature coefficient of reactivity, are being predicted satisfactorily.

Comparisons with earlier data indicate the new matrices to be a significant improvement.

During the course of this work the following papers have been issued.

Butland, A.T.D.	'LEAP AND ADDELT, a users guide to two complementary codes on the ICL-470 for calculating the scattering law from a phonon frequency function', AEEW-M1200 (1973).
Butland, A.T.D. Maddison, R.J.	'The specific heat of graphite: an evaluation of measurements', Journ. Nucl. Mats. 49, (1973/74), p.45-56.
Butland, A.T.D.	'The generation of improved thermal neutron scattering models for graphite', AEEW-R882 (internal document).

Light and Heavy Water

Sets of thermal neutron scattering matrices for H in H_2O and D in D_2O have been developed, using Nelkin and Honeck's models respectively, at seven temperatures in the range 293^{o}K to 620^{o}K. This work was carried out because previous matrices did not extend to sufficiently high temperatures and because somewhat improved calculational methods have been developed e.g. the scattering law was tabulated over a more adequate α/β mesh. In addition the latest evaluations of the free atom scattering cross-sections were used.

These latest sets have been shown to be internally consistent, and have been found to give good agreement with experimental measurements of light and heavy water total scattering cross-section and Maxwellian averaged thermal neutron diffusion parameters. In these comparisons oxygen was assumed to scatter like a free gas.

During the course of this work the following papers have been issued:

Butland, A.T.D. Chudley, C.T.	'Examination of thermal neutron scattering models for light and heavy water by comparison with diffusion and cross-section data', Journ. Brit. Nucl. Energy Soc., 1974, 13 (1) pp 99-114.
Butland, A.T.D. Oliver, S.M.	'The preparation of WIMS light and heavy water thermal scattering data (1974)', AEEW-R950.

Uranium Dioxide

Some effort has been devoted to examining the effect of crystalline binding on the temperature broadening of resonances for U in UO_2. This work has concluded that the broadening may be calculated assuming that the uranium atoms behave as a free gas, but at an effective temperature $\bar{T}$ less than 3½% higher than the thermodynamic temperature T for T $\geq$ 300^{o}K. A paper describing this work will be published shortly.

CHEMICAL NUCLEAR DATA

Introduction

It is convenient to gather together all Chemical Nuclear Data contributions under a single heading as this type of work is often collaborative in nature and is closely co-ordinated by the U.K. Chemical Nuclear Data Committee (Chairman: J.G. Cuninghame, AERE).

A. Measurements completed

1. ^{235}U fission yields in fast monoenergetic neutron fluxes (J.G. Cuninghame, Mrs. J.A.B. Goodall, H.H. Willis (AERE))

The absolute yields of 5 nuclides have been measured at neutron energies of 130, 300, 700, 900, 1300 and 1700 keV. The yields of ^{99}Mo, ^{140}Ba and ^{147}Nd are constant within standard deviations of $\pm$ 3.5%, 3.3% and 4.7% respectively over the whole energy range. Those of ^{111}Ag and ^{153}Sm increases with increasing energy as the valley of the mass yield curve rises and the wings splay out. This work is to be published in the Journal of Inorganic and Nuclear Chemistry.

2. Effect of change of angular momentum and excitation energy on the fissioning nucleus ^{239}Pu* (J.G. Cuninghame and Mrs. J.A.B. Goodall (AERE))

This work is now complete and is being prepared for submission to J. Phys. Soc. The observed large differences in scission point parameters for compound nuclei at the same excitation energy but different angular momentum is believed to be too great to be due solely to the angular momentum difference. It may be caused because there is more direct interaction when the bombarding particle is ^{3}He rather than ^{4}He.

B. Measurements in progress

1. ^{239}Pu fission yields in fast monoenergetic neutron fluxes (J.G. Cuninghame, H.H. Willis (AERE))

This is a similar series of measurements to those in A1 above, but with ^{239}Pu as the target nucleus. The results are expected in 1975.

2. Effect of change of reactor neutron spectrum on fission yields (J.G. Cuninghame, H.H. Willis (AERE))

The feasibility of measuring absolute fission yields for ^{235}U, ^{238}U and ^{239}Pu in fast reactor spectra from different parts of the Zebra core has been studied. A series of such measurements is about to begin and is expected to be completed in 1975.

3. Mass spectrometric fission yields and alpha measurements in DFR; ^{235}U (E.A.C. Crouch, I.C. McKean (AERE))

The irradiations are complete and the results of the measurements are expected in late 1974.

4. Mass spectrometric fission yields and alpha measurements in DFR; ^{238}U and ^{239}Pu (E.A.C. Crouch and I.C. McKean (AERE))

The irradiations are complete and the measurements await the availability of effort; may be completed in 1975.

5. <u>Mass spectrometric measurements of alpha in PFR</u> (E.A.C. Crouch, J.G. Cuninghame, I.C. McKean, H.H. Willis (AERE), V.M. Sinclair (DERE), D.G. Vallis (AWRE))

Samples of U and Pu isotopes are now at Dounreay and will be put into PFR for its first high power run. Results should be ready 6 months after the samples are received at the laboratories, provided effort is available to make the measurements. Note that the same measurements are being made at three different laboratories in an effort to resolve discrepancies in earlier work.

6. <u>Half-lives of ^{237}Np and ^{239}Pu</u> (K.M. Glover and F.J.G. Rogers (AERE))

Expected completion date late 1974.

7. <u>The cross-section for the production of ^{244}Cm from ^{243}Am in a fast reactor spectrum</u> (Mrs. K.M. Glover (AERE))

Following on the measurement of the production cross-section for ^{242}Cm from ^{241}Am, the ^{244}Cm production cross-section from ^{243}Am is to be measured in ZEBRA. Completion expected early 1975.

8. <u>Effect of change of angular momentum and excitation energy on the fissioning nucleus ^{208}Po*</u> (J.G. Cuninghame, J.A.B. Goodall (AERE); I.S. Grant, J. Durrell, A. Christy and J. Shea (Physics Dept., Manchester University); G.W. Newton, V.J. Robinson, J. Freeman (Chemistry Dept., Manchester University))

The nucleus ^{208}Po* is being made by the following nuclear reactions:-

$$\left.\begin{array}{l} {}^{204}\mathrm{Pb} + {}^{4}\mathrm{He} \\ {}^{196}\mathrm{Pt} + {}^{12}\mathrm{C} \\ {}^{192}\mathrm{Os} + {}^{16}\mathrm{O} \end{array}\right\} \longrightarrow {}^{208}\mathrm{Po}^{*} \xrightarrow{\text{fission}}$$

at three different excitation energies at the Harwell VEC. The reactions are being studied (a) in an on-line 3-parameter (E_1, E_2, T) fission fragment experiment and (b) by fast chemical separation. It is hoped to get information on such scission point properties as charge distribution, mass distribution, kinetic energy distribution and prompt neutron distribution as a function of mass. For the first time on-line physical and off-line radiochemical measurements are being compared directly in simultaneous irradiations. The work is about half complete.

9. <u>Fission yield measurements</u> (V.M. Sinclair, W. Davies (DERE))

Two separate sets of absolute mass-spectrometric fission yield measurements are in progress. In both gramme quantities of ^{235}U and ^{239}Pu, together with milli-gramme amounts of ^{240}Pu are being used.

The capsules from the first set have already been irradiated in D.F.R. and are awaiting the final chemical analysis. Those from the second will be irradiated in P.F.R. in 1975.

In both sets burn-ups in the range 10-20% are expected for both uranium and plutonium and the fission products to be measured will include the Nd isotopes, ^{90}Sr, ^{137}Cs and ^{144}Ce.

C. Compilations and evaluations

1. Independent fission yields (E.A.C. Crouch (AERE))

An evaluation of all known fractional and cumulative independent yields, and a calculation of those unknown in fission of ^{232}Th, ^{233}U, ^{235}U, ^{238}U, ^{239}Pu, ^{240}Pu and ^{241}Pu, has been completed and is awaiting final recommendation by the Chemical Nuclear Data Committee, probably in May 1974.

2. Objective evaluation of all fast fission yields (E.A.C. Crouch (AERE))

This paper brings up to date the subjective yield evaluation already issued as AERE-R 7394 and applies constraints determined by the physics of fission to them. Will be issued after recommendation by the Chemical Nuclear Data Committee, probably in mid-1974.

3. α energies and intensities (F.J.G. Rogers (AERE))

Will be issued after recommendation by the Chemical Nuclear Data Committee, probably in mid-1974.

4. Fast fission yield "evaluation of evaluations" (J.G. Cuninghame (AERE))

A complete review paper on fast yields was prepared for the IAEA Panel on Fission Product Nuclear Data, Bologna, November 1973 and issued as AERE-R 7548, 1973.

5. βγ decay schemes for all fission products (A. Tobias (CEGB))

A CNDC recommended document has been published as CEGB report RD/B/M2669, 1973.

6. βγ decay schemes and other fission data (N.R. Large (AERE); B.S.J. Davies (CEGB); D.G. Vallis (AWRE); M.F. James (AEEW))

The above sub-committee of the CNDC is preparing a complete file in ENDF/BIV format of fission product and actinide chemical nuclear data. The first part of the work consists of incorporating the existing Tobias data (C5 above) and it is hoped that Crouch's fission yield data will soon follow, as well as Rogers' α-data. Eventually it is hoped to include other non-fission product decay data. The γ energy and intensity part of the file is being incorporated with the DIODE γ-analysis computer library.

The ultimate aim is to hold and keep up-to-date a complete UK file in ENDF/B format of all "chemical" nuclear data and to issue periodic printed listings from it, but the work is very seriously hampered by shortage of effort and no completion date can be given.

D. Publications

"Absolute yields in the fission of ^{235}U by monoenergetic neutrons of energy 130-1700 keV".
J.G. Cuninghame, Mrs. J.A.B. Goodall, H.H. Willis.
J. Inorg. and Nucl. Chem. in press 1974.

"Data for calculation of γ-radiation spectra and β-heating from fission products (Rev 3)".
A. Tobias, CEGB RD/B/M2669 1973.

"Review of fission product yield data for fast neutron fission".
J.G. Cuninghame, AERE-R 7548 1973.

NATIONAL PHYSICAL LABORATORY

DIVISION OF RADIATION SCIENCE

(Superintendent: Dr. P.J. Campion)

1. Calibration Services

The NPL maintains standards of neutron flux density and facilities for the calibration of neutron sources. Extension and improvement of the standards available including international intercomparisons with other national laboratories is a continuing process. Details of services available and their cost are described in a booklet called Measurement Services, available free of charge from the Division of Radiation Science, National Physical Laboratory.

2. Standards of neutron flux density

Alternative methods of measurement of neutron flux density are being developed as a means of investigating systematic errors in existing standards.

2.1 Intermediate energy (J.B. Hunt)

The existing secondary standard long counter calibration is derived from a combination of results obtained with radioactive neutron sources calibrated in the manganese sulphate bath and from comparisons of the yield from the Li(p,n) reaction using the long counter and a collimated vanadium sulphate bath.

A hydrogen proportional counter is being built to measure neutron flux in this energy range in terms of the hydrogen cross-section thus establishing a new primary standard. In addition the neutron flux will be measured in terms of the ^{57}Co activity produced by the ^{57}Fe(p,n) reaction in order to provide an alternative absolute calibration of the long counter.

2.2 Fast neutron energies (T.B. Ryves, K.J. Zieba)

For neutrons in the D-D energy range the existing long counter calibration is provided by results obtained with neutron sources with extended spectra which have been calibrated in the manganese sulphate bath. A proton recoil telescope consisting of two proportional counters and a semi-conductor counter has been built in order to measure the neutron flux in terms of the hydrogen cross-section. The possibility of using associated particle counting of the associated ^{3}He particles from the D-D reaction is being investigated.

For 14.8 MeV neutrons from the D-T reaction using the low energy SAMES accelerator, the ^{56}Fe(n,p) reaction has been measured using a proton recoil counter for the measurement of the neutron flux density. This cross-section is now in use as a secondary standard for routine calibrations at this neutron energy.

A new proton telescope has been designed to measure neutrons in the 12-20 MeV energy range using D-T neutrons from the Van de Graaff accelerator. The results will be compared with those obtained from counting the associated alpha particles from the D-T reaction.

2.3 Neutrons below 10 keV (E.J. Axton and A.G. Bardell)

A method is being developed to provide neutron monitor calibrations in this energy range. Neutrons will be produced in a small water bath by the $^{7}Li(p,n)$ reaction and a filter difference method used to select neutron energy bands from the escaping slowing down flux. The method relies on Monte-Carlo calculated spectra combined with BF_3 counter measurements of the neutron density.

3. Reference standard for neutron radiotherapy (E.J. Axton, A.G. Bardell, V. Lewis)

A small D-T accelerator is being built to provide a collimated beam of 14.8 MeV neutrons as part of a programme to establish a National reference standard, based on the cavity ionization chamber principle, for the measurement of neutron absorbed dose.

4. Neutron spectroscopy (V. Lewis)

A proton recoil spectrometer is being developed for the purpose of measuring the neutron energy spectrum in the collimated 14.8 MeV neutron beam.

The programme includes remeasurement of the energy spectra of some well known neutron sources, e.g. Am-Be and ^{252}Cf.

5. $\bar{\nu}$ for Spontaneous fission of ^{252}Cf (E.J. Axton and A.G. Bardell) [Relevant to Request Numbers: 691359, 691824, 712119, 714033, 714034]

The apparent discrepancy of about 0.5% between results obtained with samples of different age as mentioned in the previous report remains unexplained. No further measurements are contemplated with those samples in view of their age. A programme of Monte Carlo calculation is in progress to obtain new assessments for the manganese bath corrections for neutron escape, thermal neutron capture in the source assembly and fast neutron capture in oxygen and sulphur. Results obtained so far indicate that whilst small changes may be made in the individual corrections the overall effect on the NPL value for $\bar{\nu}$ for ^{252}Cf will be negligible.

A possible explanation of the apparent conflict between absolute measurements of $\bar{\nu}$ for ^{252}Cf and of η may be found in the g values used to link the two sets of measurements. A review of g values is therefore necessary before the IAEA review panel can finalize the input data to the 2200 ms^{-1} least squares fit.

6. Nuclear decay scheme measurements

These measurements are limited to those decay scheme parameters that are required either for accurate measurements of standards of radioactivity or by users of these standards. Recently measurements have been made of the half-life of ^{51}Cr (1), the total internal conversion coefficients in the decay of ^{87m}Sr and ^{113}In (2,3) and the γ-branching ratio in the decay of ^{7}Be (4).

---

(1) Measurement Services, Radiation Science, 1974.

(2) I.W. Goodier, F.H. Hughes and M.J. Woods. Int. J. Appl. Radiat. Isotopes. 19, 795 (1968).

(3) I.W. Goodier, F.H. Hughes and M.J. Woods. Ibid 21, 678 (1970).

(4) To be published in Int. J. Appl. Radiat. Isotopes.

KELVIN LABORATORY, UNIVERSITY OF GLASGOW

(Director: Prof. G.R. Bishop)

Electrofission of U-238 (J.M. Reid, J.M. Hendry (Univ. of Glasgow), A.C. Shotter, D. Branford and J.S. Barton (Univ. of Edinburgh))

A study of the electrofission of ^{238}U is in progress using the electron beam of the Kelvin Laboratory Linear Accelerator. Silicon surface barrier detectors measure singly and in coincidence the energies of fission fragments emitted at 90° to the electron beam from a deposit of uranium on a thin nickel backing. Spectra have been measured at various incident electron energies. As shown in Figure 18, they exhibit the double peak characteristic of fission fragments. The peak to valley ratio taken as a measure of asymmetric to symmetric mass division enables a comparison to be made with photofission results obtained by chemical analysis (Fig. 19). The electrofission process proceeding via a virtual proton is expected to show similarities to the photofission process. However, the differences in the absorption of virtual as compared to real photons will ensure a different mixture of excited states of the fissile nucleus in the electron induced process.

A study of the average fragment kinetic energy released as a function of incident electron energy (Fig. 20) shows a monotonic increase. This behaviour contrasts with particle induced fission where additional bombardment energy results usually in increased neutron emission and a reduction in fragment kinetic energy.

Further data on $e(^{238}U,f)e'$, in process of analysis, appears to be confirming these preliminary results.

Neutron time-of-flight experiments (G.I. Crawford, S.J. Hall, J.D. Kellie, J. McKeown, D.B.C.B. Syme)

Since compilation of our 1972 report, the efforts of the group have been devoted primarily to high resolution measurements of total neutron cross-sections in the energy range 0.2 MeV - 10 MeV. Some advances in neutron detector techniques and system capability have been incorporated. Preliminary steps have been taken in the construction of a gas scintillator chamber to allow high resolution studies of (n,fiss) and (n,α) interactions.

The measurements of the total cross-section of La, Ce, Pr, Nd, Sm, Gd, Dy, Ho, Er and Yb reported previously(1) have now been completed and the results are shown in Figs. 21 to 24. The data were obtained with the Kelvin Laboratory linear accelerator using a 103 m flight path and the total time resolution of the measurements was 5 nsec.. The error bars on the figures refer to the statistical errors only and the solid lines are calculated values obtained from optical model fits using the generalised optical potential of Wilmore and Hodgson. In general the fits are in reasonably good agreement with the magnitudes of the measured cross-sections but they agree less well with their energy dependence.

---

(1) UKNDC(73)P53, EANDC(UK)-151L, INDC(UK)20L.

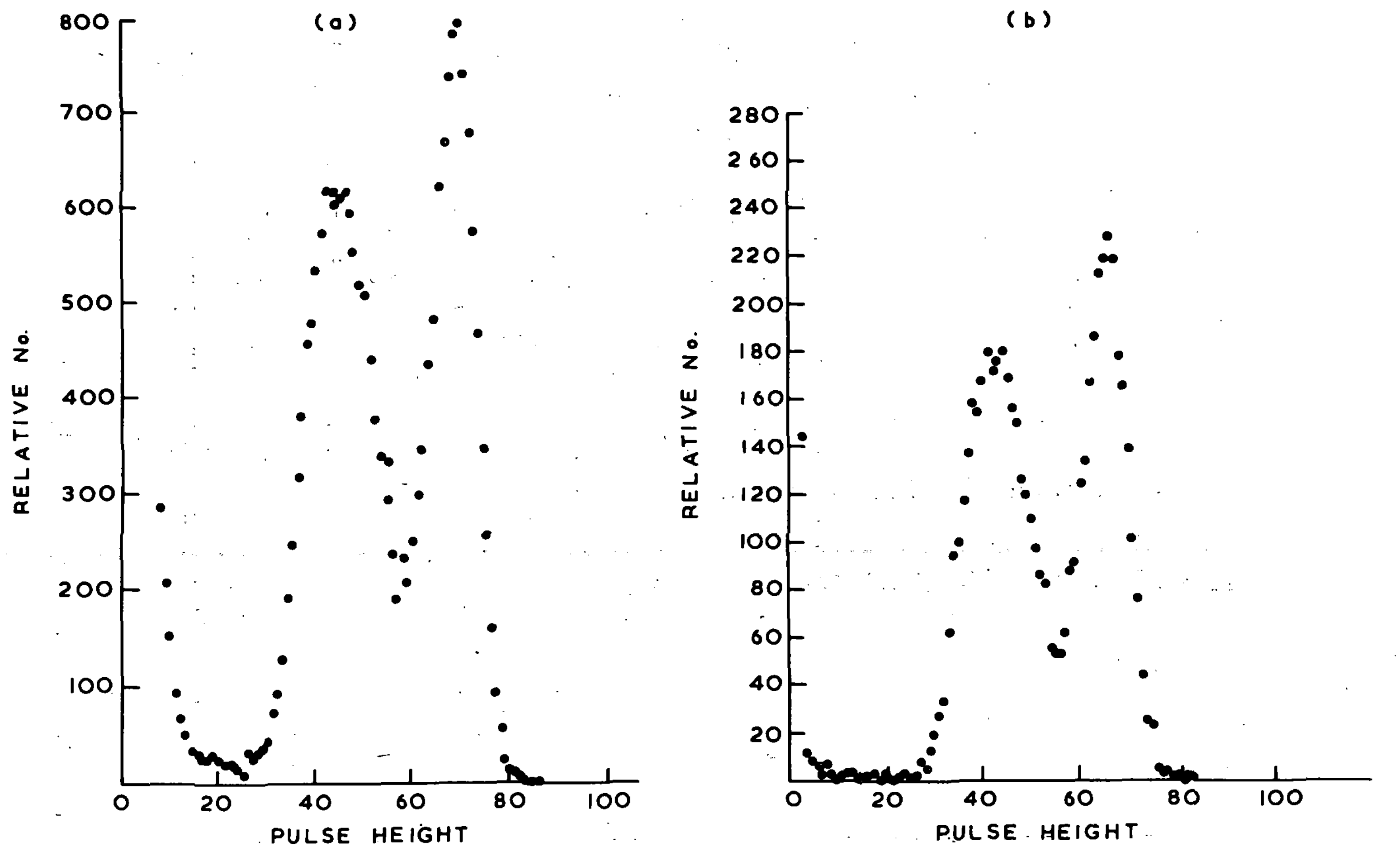

Fig. 18 The energy spectrum of signals from one of the fission detectors: (a) With no coincidence requirement, (b) Coincidence required between the detectors on either side of the fission foil

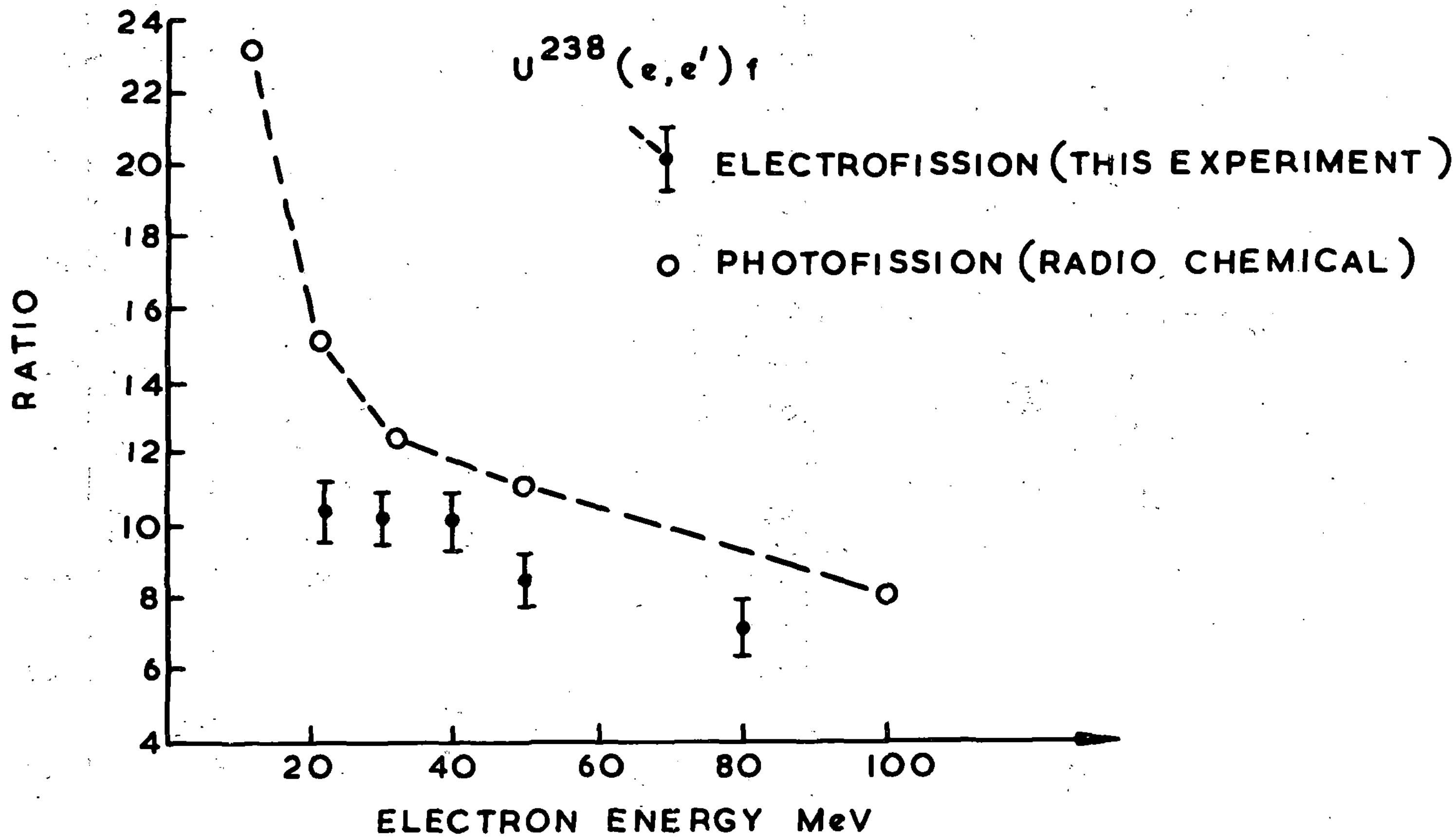

Fig. 19 Ratio of asymmetric to symmetric mass division as a function of incident electron energy

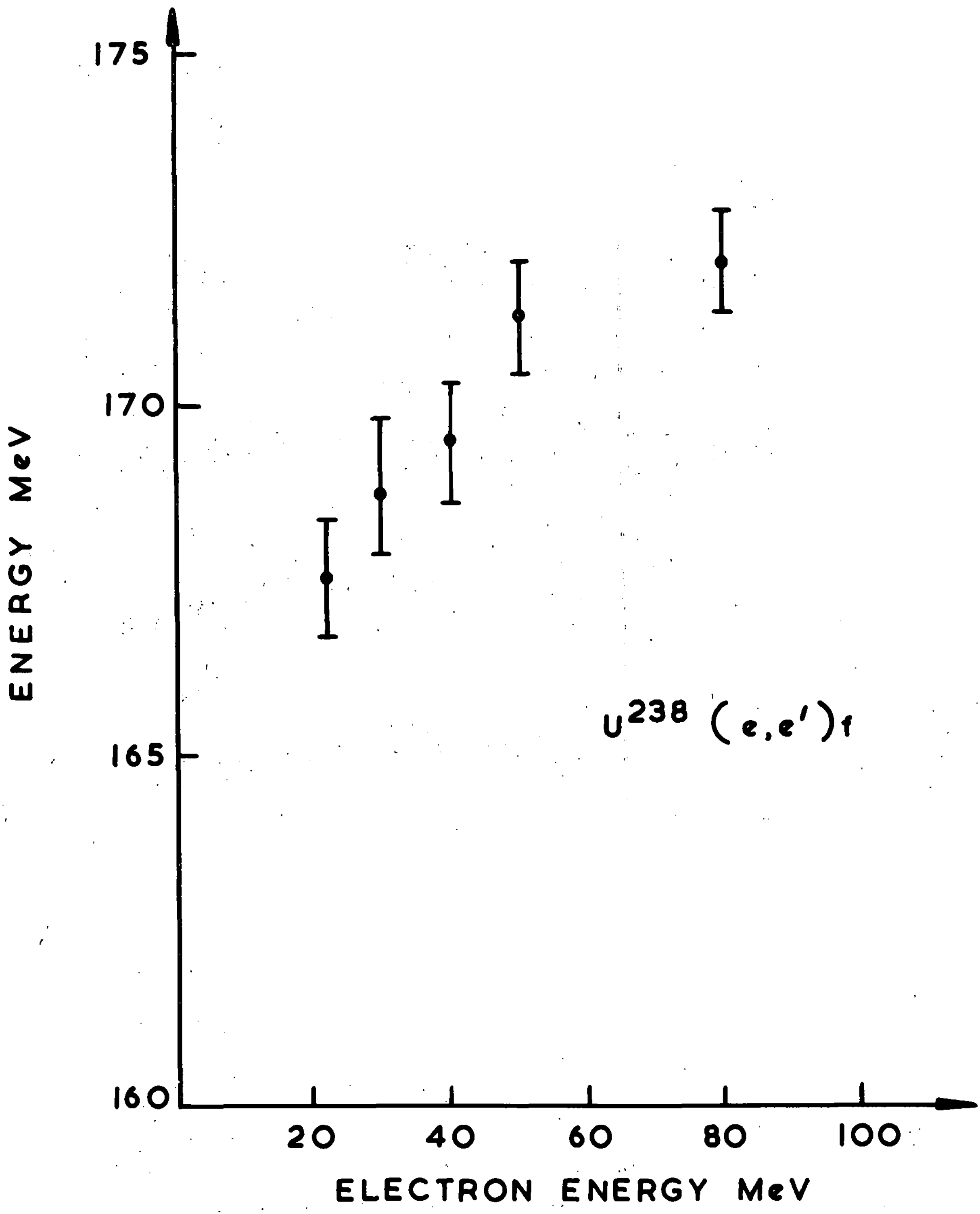

Fig. 20 Average kinetic energy released for electrofission of U-238 as a function of incident electron energy

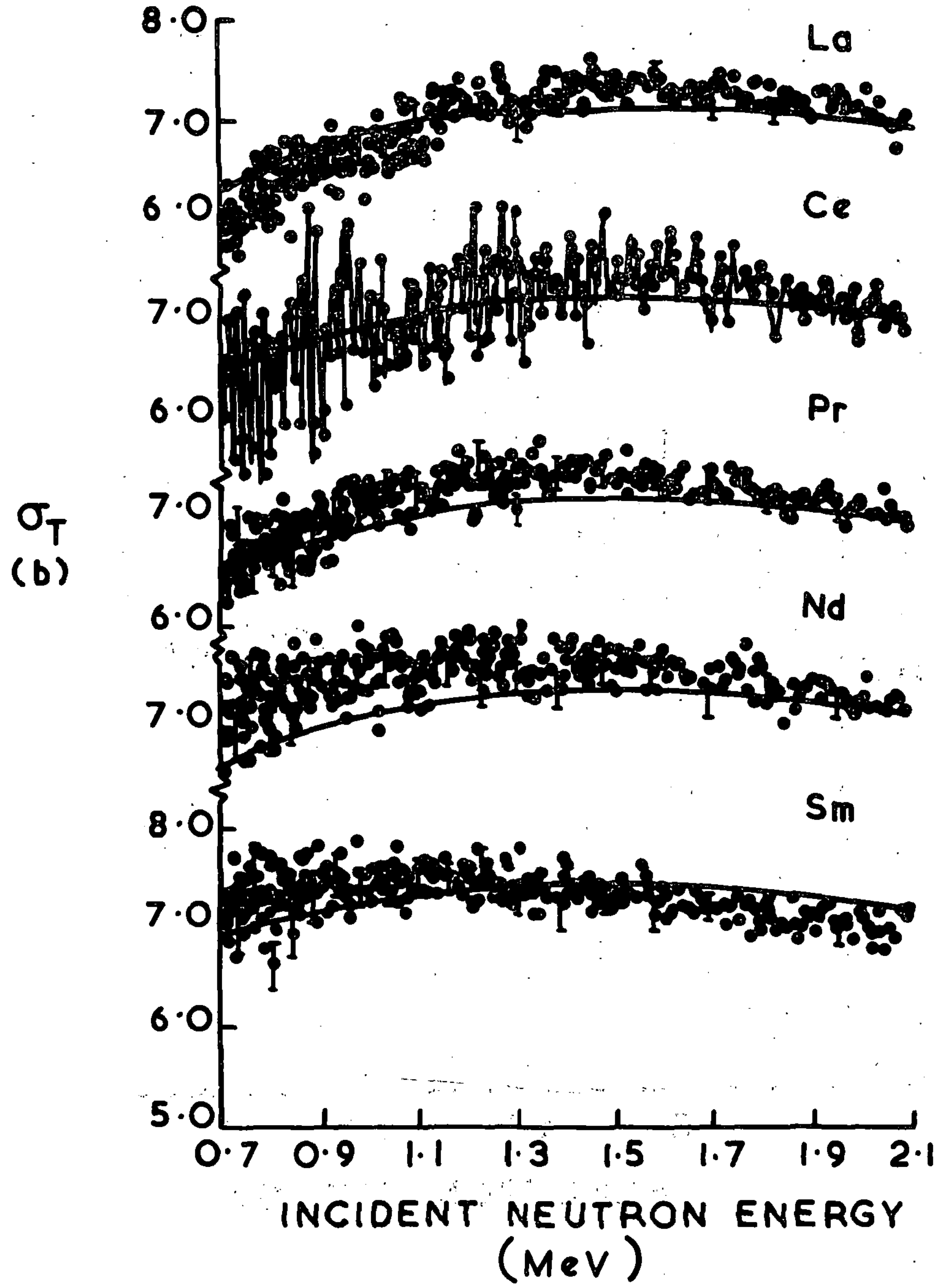

Fig. 21 The total cross-sections of La, Ce, Pr, Nd and Sm between 0.7 and 2.1 MeV

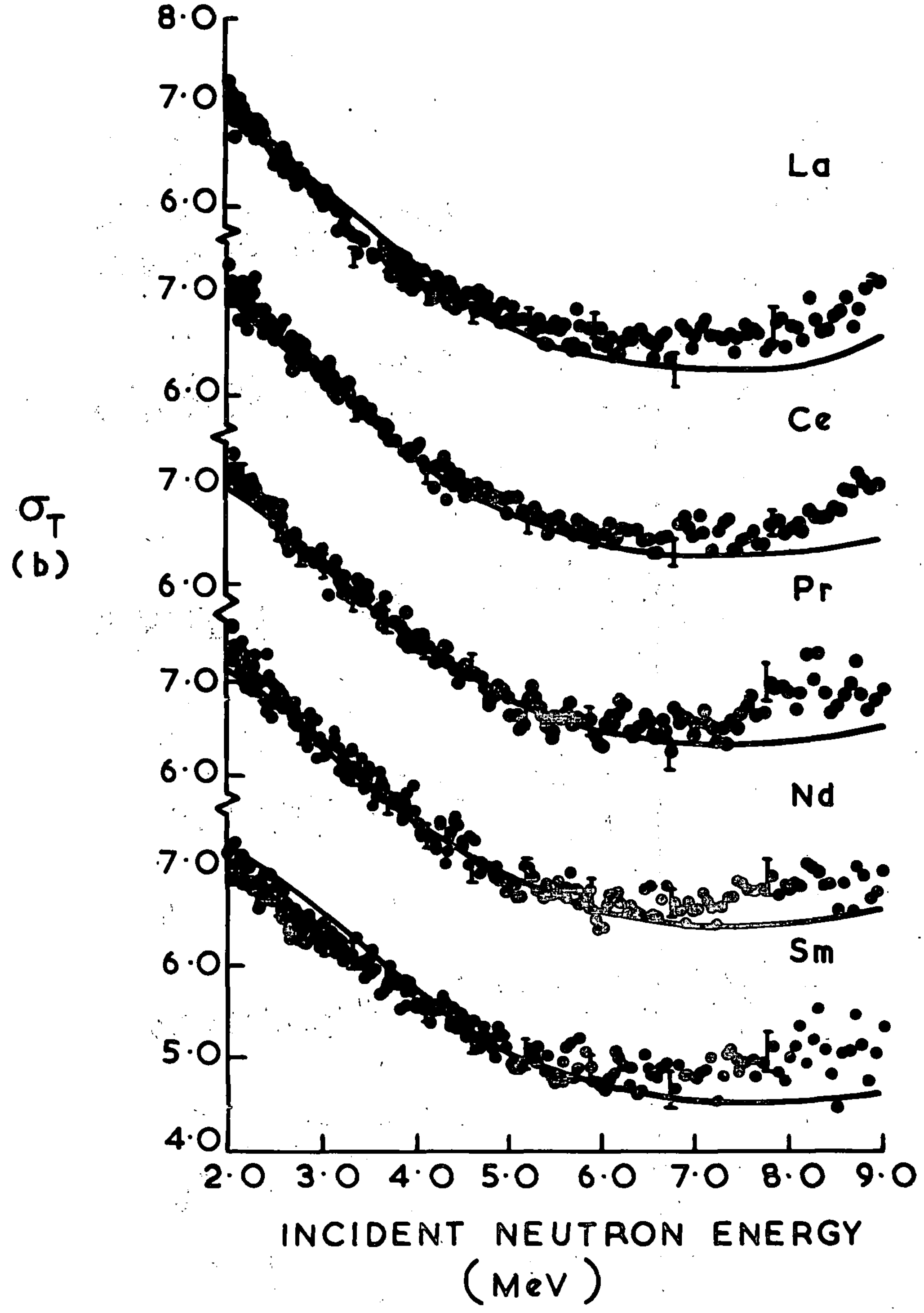

Fig. 22 The total cross-sections of La, Ce, Pr, Nd and Sm between 2 and 9 MeV

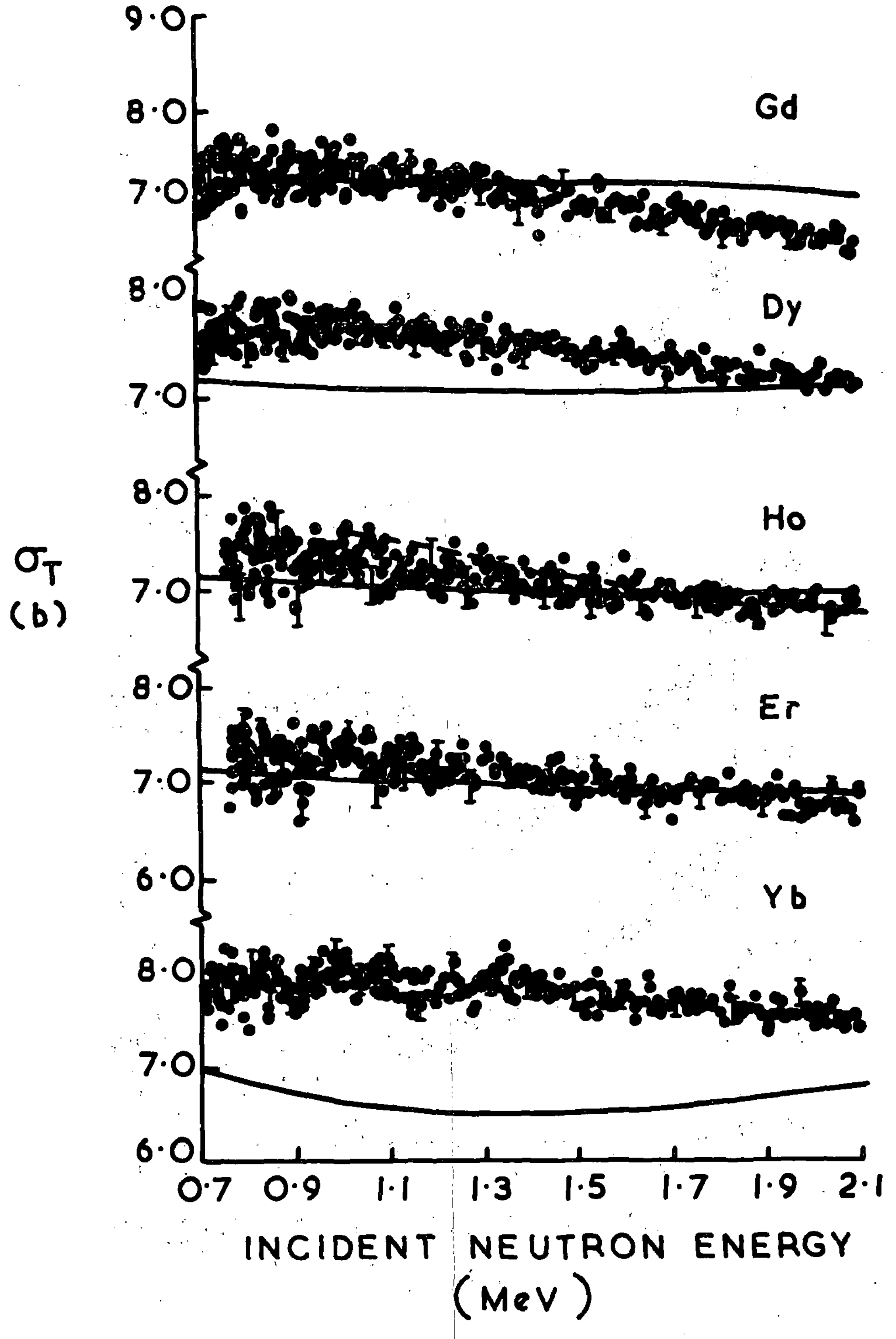

Fig. 23 The total cross-sections of Gd, Dy, Ho, Er and Yb between 0.7 and 2.1 MeV

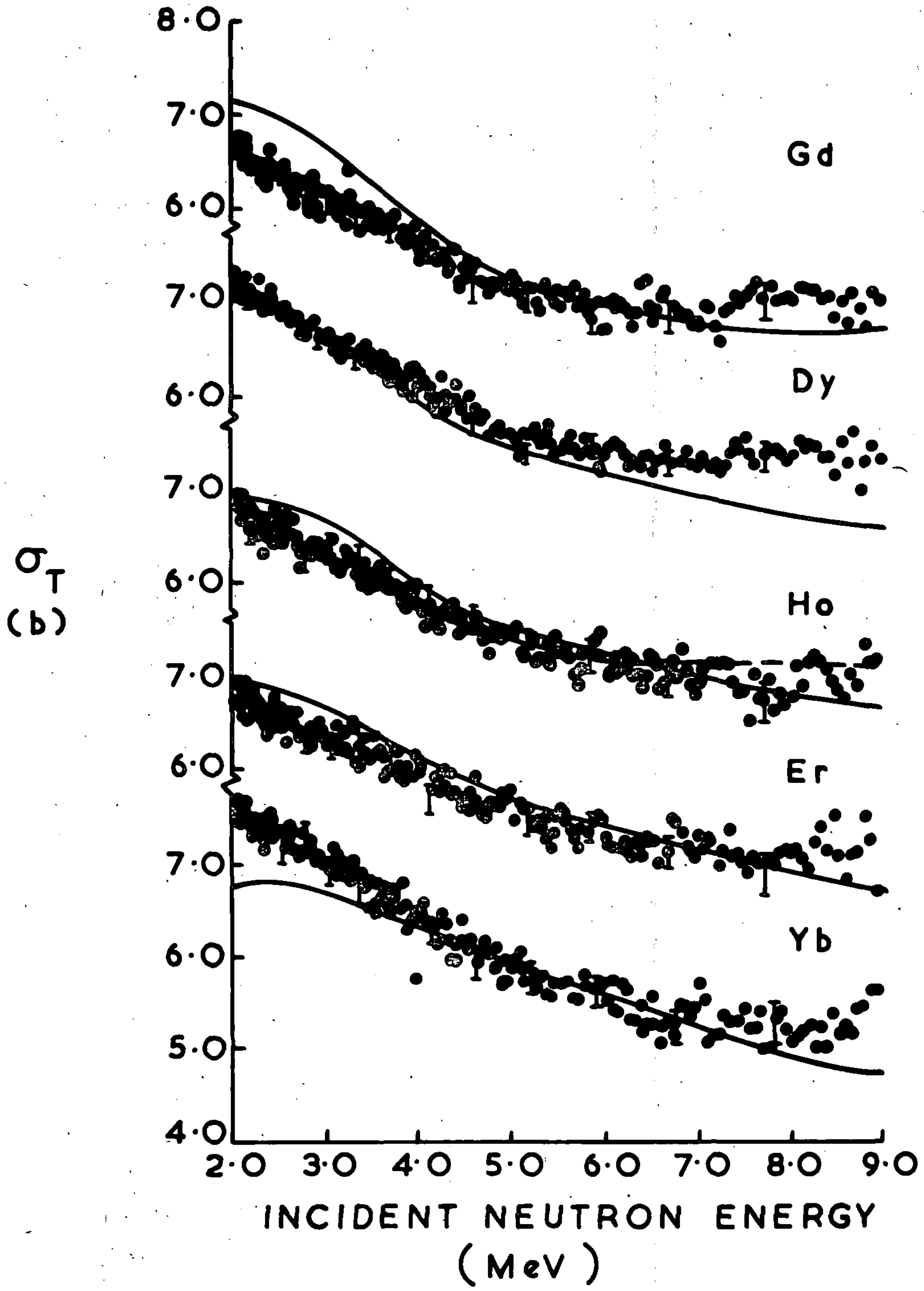

Fig. 24 The total cross-sections of Gd, Dy, Ho, Er and Yb between 2 and 9 MeV